Dissecting Olfactory Circuits in Drosophila

Dissertation Advisor: Dr. Rachel Wilson Wendy Wing-Heng Liu

Dissecting Olfactory Circuits in *Drosophila*

Abstract

Drosophila is a simple and genetically tractable model system for studying neural circuits. This dissertation consists of two studies, with the broad goal of understanding sensory processing in neural circuits using *Drosophila* as a model system.

A key tool in the study of neural circuits is the ability to transiently inactivate specific neurons. In *Drosophila*, the current techniques for doing this are limited. The first study describes a novel technique for transient and specific inactivation of *Drosophila* neurons *in vivo* using a native histamine-gated chloride channel (Ort). Since many regions of the *Drosophila* brain are devoid of histaminergic neurons, Ort could be used to artificially inactivate specific neurons in these regions. We found that histamine effectively silenced neurons misexpressing Ort. Ort also performed favorably in comparison to the available alternative effector transgenes. Thus, Ort misexpression is a useful tool for probing functional connectivity among *Drosophila* neurons.

Understanding the physiological effects of neurotransmitters is critical to deciphering neural circuit function. Although glutamatergic neurons are abundant in the *Drosophila* brain, the effects of glutamate are largely unknown. The second study investigated the role of glutamate in the olfactory system. We found that glutamate acts as an inhibitory neurotransmitter, broadly similar to the role of GABA in this circuit. The existence of two parallel inhibitory transmitter systems may increase the range and flexibility of synaptic inhibition.

Together these studies enhance our understanding of how sensory stimuli are represented and processed in the brain.

Table of Contents

List of Figures

Acknowledgements

I am deeply grateful for all the people who have generously offered any kind of help, guidance, and encouragement, no matter how small. First and foremost, I would like to thank my advisor, Rachel Wilson. Although I knew close to nothing about neuroscience when I joined the lab, she was very patient in teaching me both conceptual and technical knowledge. She is fully committed to the success of everyone in the lab, and I am always amazed by how far she would go to help her students. I am inspired by her meticulous thinking, creativity, and sincere generosity. I have grown so much as a scientist and as a person through my interactions with her, for which I am truly grateful.

I want to thank all the members of the Wilson lab for contributing to a fun and collaborative work environment. I thank Tony Azevedo, Allison Baker, Joe Bell, Mehmet Fisek, Betty Hong, James Jeanne, Kathy Nagel, Willie Tobin, John Tuthill and other Wilson lab alumni for being wonderful people to work with, and for sparking interesting conversations and laughter.

I am very grateful to Ofer Mazor for providing engineering expertise which was critical to the work on thermosensory circuits. He is never short of interesting ideas and I greatly benefited from my discussions with him. It was a pleasure collaborating with him to build the jet micro-thermode.

I thank Betty Hong, Man Yan Wong, Stephen Zhang and Zhihua Li for their generous advice and assistance with generating transgenic flies. I thank Dragana Rogulja for kindly allowing me to perform molecular biology experiments in her lab and for sharing reagents with us.

I thank Bruce Bean, David Corey, Qiufu Ma, Chinfei Chen and Bernardo Sabatini for serving on my dissertation advisory committee and for providing valuable feedback.

I am grateful to my parents and sister for their unconditional love and encouragement throughout the years. They were always there for me. The most wonderful thing that happened during graduate school was getting married to my husband Wallace. He never fails to bring joy into my life and has helped me sacrificially in ways small and big. Finally and most importantly, I am grateful to God, the giver of all good things, and without whom nothing would be possible. *Soli Deo Gloria*.

CHAPTER 1: General Introduction

Drosophila as a model for studying neural circuits

Ever since Thomas H. Morgan discovered the *white* eye pigment mutation at the turn of the twentieth century, *Drosophila* has been a choice model system for studying many facets of biology. While early research in *Drosophila* focused on heredity, genetic approaches were developed that enabled important discoveries in nervous system development and function, such as the identification of pathways involved in neurogenesis (Ho and Scott, 2002), neuronal migration (Gaiano, 2008), and growth cone guidance (Charron and Tessier-Lavigne, 2007), as well as the discovery of many ion channels (Montell et al., 1985; Salkoff et al., 1992; Tempel et al., 1987; Warmke and Ganetzky, 1994) and proteins involved in synaptic transmission (Littleton et al., 1994; Richmond and Broadie, 2002; van der Bliek and Meyerowitz, 1991). The field of behavioral neurogenetics started in the fifties and sixties when Seymour Benzer used forward genetic screens to isolate behavioral mutants, leading to the identification of genes that control complex behaviors such as circadian rhythms, courtship, and learning and memory (Benzer, 1973). With the development of functional imaging and single-cell electrophysiology, neural activity in the *Drosophila* brain can be monitored *in vivo* (Cao et al., 2013; Ng et al., 2002; Tian et al., 2009; Wang et al., 2003; Wilson et al., 2004). This enables us to study how information is represented in neural circuits and what computations are being performed.

There are several advantages of using the fruit fly to study neural circuits. One obvious advantage is the arsenal of genetic tools available. A key genetic technique is the use of binary expression systems, such as the GAL4/UAS system, to label and manipulate defined neuronal populations (Venken et al., 2011). Other practical advantages include having a short generation time, which allows large-scale genetic and behavioral experiments to be performed efficiently,

and having a fully sequenced and annotated genome. More fundamentally, the *Drosophila* brain offers a useful compromise between numerical simplicity and richness. There are around 100,000 neurons in *Drosophila*, 1000-fold fewer than mice. This simplicity means that it may be feasible in some cases to comprehensively map all the elements of a neural circuit. *Caenorhabditis elegans* has an even simpler nervous system with 302 neurons, but its behavioral repertoire is more limited. Finally, many *Drosophila* circuits are genetically hard-wired (Berdnik et al., 2006; Hiesinger et al., 2006; Jefferis et al., 2001). Neural identity and connectivity are relatively stereotyped, allowing for meaningful comparisons across flies and experimental conditions.

The work described in this dissertation uses *Drosophila* as a model for understanding how sensory circuits process information. Chapter 3 describes work on olfactory circuitry. Chapter 2 introduces a new technique that has potential applications in studying a variety of neural circuits in *Drosophila*, including sensory circuits.

Tools for silencing neuronal activity in *Drosophila*

Understanding information processing in neural circuits requires characterization of the neurons involved and their connections, as well as the ability to manipulate their activity. In particular, by silencing groups of neurons one can identify those that are necessary for certain behaviors, and reveal functional connectivity between neurons.

One way of removing neurons from a circuit is to cause cell death. The GAL4/UAS system can be used to target expression of toxins or genes that initiate programmed cell death to specific neuron populations. Expression of Diphtheria toxin and Ricin kills cells by inhibiting protein synthesis (Bellen et al., 1992; Kunes and Steller, 1991; Moffat et al., 1992), while expression of the proapoptotic genes *grim*, *reaper*, or *hid* initiate programmed cell death (Zhou et

al., 1997). The efficiency of cell killing depends on neuron type and developmental stage. Hence, coexpression of a visible reporter is necessary to confirm that the target cells have been killed.

In cases where cell death is undesirable, silencing of neurons can be achieved by blocking synaptic transmission. Expression of the light chain of tetanus toxin cleaves neural synaptobrevin and blocks neurotransmitter release (Sweeney et al., 1995). Since tetanus toxin targets a neuron-specific protein, it should only affect neurons. However, it is constitutively active, and chronic expression could lead to compensatory changes in the circuit. Alternatively, neurotransmission can be blocked acutely by expressing *shibire*^{ts1}, a temperature-sensitive dominant-negative form of dynamin, which is required for synaptic vesicle endocytosis. At the restrictive temperature (30°C), vesicular release stops in neurons expressing *shibire*^{ts1} because the supply of vesicles is depleted (Kosaka and Ikeda, 1983). While acute temporal control is a virtue of this technique, the elevated restrictive temperature may affect neuronal physiology. Overexpression of *shibire*^{ts1} also causes a reduction of vesicular release and accumulation of microtubules in some cells at permissive temperatures (Gonzalez-Bellido et al., 2009).

Blocking membrane depolarization is another way to silence neurons. This is commonly achieved by overexpressing a potassium channel, which would lower the resting membrane potential or increase shunt current. Potassium channels that have been used for this purpose include Kir2.1, a mammalian inward rectifying potassium channel, and dORK, a two-pore potassium leak channel (Nitabach et al., 2002; Paradis et al., 2001).

More recently, halorhodopsin, a light-activated chloride pump, has been used in *Drosophila* to hyperpolarize neurons with high temporal and spatial precision (Inada et al., 2011). However, it has a low conductance, and requires high levels of expression to be effective (Fenno et al., 2011).

Other than shibire^{ts1} and halorhodopsin, all other methods for silencing *Drosophila* neurons work on longer timescales of hours to days. In many experiments, transient silencing is desirable, as chronic manipulations may cause developmental changes and homeostatic compensation. In Chapter 2, I will describe a novel method for transient and specific inactivation of *Drosophila* neurons *in vivo* using a native histamine-gated chloride channel.

The *Drosophila* olfactory system

Olfaction begins when odors bind to receptor proteins on the surface of olfactory receptor neurons (ORNs) in the antenna. ORNs project their axons to the antennal lobe, where they synapse onto second-order principal neurons called antennal lobe projection neurons (PNs). The antennal lobe is divided into ~50 glomeruli. All the ORNs that express the same odorant receptor project to the same glomerulus, and most individual PNs extend a dendrite into only a single glomerulus, and thus receive direct input from only one type of ORN (Vosshall and Stocker, 2007). PNs then send axons to higher olfactory brain regions. Like most principal neurons in the *Drosophila* brain, ORNs and PNs release the neurotransmitter acetylcholine (Stocker, 1994). Whereas each PN is restricted to one glomerulus, the role of local neurons (LNs) in the antennal lobe is to mediate interactions between glomeruli. Some individual LNs innervate most or all glomeruli, while other LNs innervate just a few glomeruli (Chou et al., 2010b). LNs receive excitatory input from ORNs and/or PNs, and they inhibit ORN axons and/or PN dendrites (Olsen and Wilson, 2008a; Root et al., 2008; Wilson et al., 2004). LNs also synapse onto each other (Huang et al., 2010; Yaksi and Wilson, 2010).

LNs in this circuit are highly diverse in their neurotransmitter profiles and connectivity (Chou et al., 2010b). Whereas about two-thirds of LNs release the inhibitory neurotransmitter GABA, the remaining one-third release glutamate. There is a large literature on GABAergic LNs

in this circuit (Chou et al., 2010b; Ng et al., 2002; Olsen and Wilson, 2008a; Wilson and Laurent, 2005b). However, nothing is known about the role of glutamatergic LNs in this circuit, and indeed almost nothing is known about the action of glutamate in the *Drosophila* brain, although glutamatergic neurons are abundant (Daniels et al., 2008). In Chapter 3, I describe the effect of glutamate on antennal lobe neurons and the functional role of glutamatergic neurons in olfactory processing.

CHAPTER 2:

Transient and specific inactivation of *Drosophila* neurons in vivo using a native ligand-gated ion channel

---

The work in this chapter has been published as:

W.W. Liu & R.I. Wilson (2013) Transient and specific inactivation of *Drosophila* neurons in vivo using a native ligand-gated ion channel. *Current Biology* 23:1202-8.

I performed the experiments and analyzed the data. Both I and R.I.W. designed the experiments and wrote the paper.

Summary

A key tool in neuroscience is the ability to transiently inactivate specific neurons on timescales of milliseconds to minutes. In *Drosophila*, there are two available techniques for doing this (*shibire*^{ts} and halorhodopsin (Berni et al., 2012; Inada et al., 2011; Kitamoto, 2001)), but both have shortcomings (Fenno et al., 2011; Gonzalez-Bellido et al., 2009; Kitamoto, 2002; Luo et al., 2008; Simpson, 2009; Venken et al., 2011). Here we describe a complementary technique using a native histamine-gated chloride channel (Ort). Ort is the receptor at the first synapse in the visual system. It forms large-conductance homomeric channels that desensitize only modestly in response to ligand (Pantazis et al., 2008). Many regions of the central nervous system are devoid of histaminergic neurons (Nassel, 1999; Pollack and Hofbauer, 1991), raising the possibility that Ort could be used to artificially inactivate specific neurons in these regions. To test this idea, we performed *in vivo* whole-cell recordings from antennal lobe neurons misexpressing Ort. In these neurons, histamine produced a rapid and reversible drop in input resistance, clamping the membrane potential below spike threshold, and virtually abolishing

spontaneous and odor-evoked activity. Every neuron type in this brain region could be inactivated in this manner. Neurons that did not misexpress Ort showed negligible responses to histamine. Ort also performed favorably in comparison to the available alternative effector transgenes. Thus, Ort misexpression is a useful tool for probing functional connectivity among *Drosophila* neurons.

Results

Many regions of the *Drosophila* central nervous system contain no histaminergic fibers, or else only sparse histaminergic innervation (Fig. 2.1). The antennal lobe is one region that contains no histaminergic innervation, and it is one of the best-studied regions of the *Drosophila* brain. For this reason, we chose antennal lobe neurons for testing the effect of histamine on Ort-misexpressing neurons.

There are two major cell types in the antennal lobe: projection neurons (PNs) and local neurons (LNs). About two-thirds of antennal lobe LNs are GABAergic, and about one-third are glutamatergic (Chou et al., 2010a; Das et al., 2011a). We targeted expression of Ort to PNs and LNs with the Gal4/UAS system, using Gal4 lines that drive expression specifically in these cell types. We performed targeted *in vivo* patch clamp recordings from these cells. In order to target our electrodes to the Ort+ neurons, we co-expressed CD8:GFP along with Ort.

In the absence of histamine, the electrophysiological properties of Ort+ neurons were no different from those of Ort- neurons (i.e., cells recorded in flies that lacked the *UAS-ort* transgene). The resting membrane potential of these cells (-64±1 mV) was not significantly different from controls (-64±2 mV, p=0.52, n=8 and 5, t-test). Similarly, the input resistance of these cells (920±130 MΩ) was not significantly different from normal (1040±150 MΩ, p=0.58, n=8 and 5, t-test)

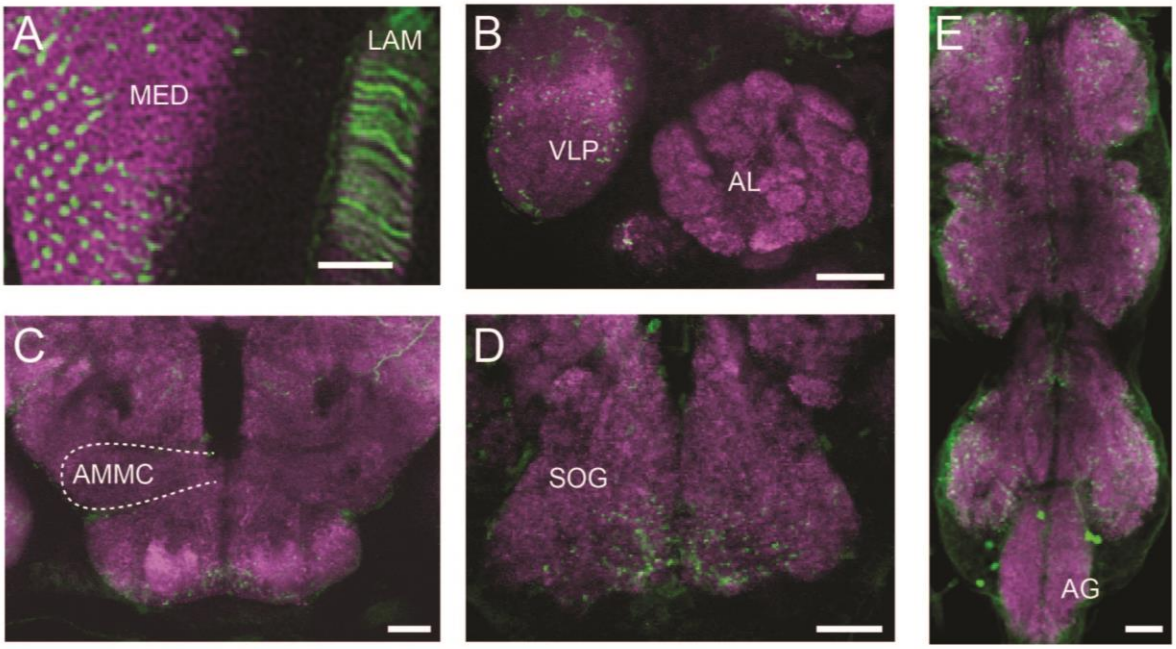

Figure 2.1: Histamine immunoreactivity in selected regions of the Drosophila central nervous system.

(A) As expected, photoreceptors are histamine immunopositive; this image shows photoreceptor terminals in the medulla (MED) and lamina (LAM) of the optic lobe.
(B) The antennal lobe (AL) is devoid of histaminergic fibers, while the ventrolateral protocerebrum (VLP) is densely innervated.
(C) The antennal mechanosensory and motor center (AMMC, outlined by dashed line) is devoid of histamine immunoreactivity.
(D) Most of the subesophageal ganglion (SOG) contains no histamine immunoreactivity, except for the ventral edge, which is densely labeled.
(E) Histaminergic fibers sparsely innervate the three pairs of neuromeres in the thoracic ganglion, but are absent from the abdominal ganglion (AG).

In addition, we observed that the mushroom body and central complex were also devoid of histamine immunoreactivity. All images are z-projections through depths of several microns. Histamine immunoreactivity is in green, with neuropil (nc82 immunoreactivity) in magenta. See Experimental Procedures for details. Scale bars = 20 μm.

Upon bath application of histamine, Ort+ neurons were potently inhibited. Odor-evoked activity was almost completely suppressed, and this was true of both Ort+ PNs and Ort+ LNs (Fig. 2.2A-C). The effects of histamine on Ort+ neurons were dose-dependent and consistent with the known sensitivity of Ort to histamine (Gengs et al., 2002; Pantazis et al., 2008; Skingsley et al., 1995; Zheng et al., 2002). At the highest dose (100 μM), histamine completely eliminated all spiking, and substantially reduced odor-evoked depolarization (Fig. 2.2B,C). Importantly, histamine had essentially no effect on the odor responses of PNs and LNs recorded in flies that lacked the *UAS-ort* transgene, even at the highest histamine concentration (Fig. 2.2D,E).

The effects of histamine are consistent with the opening of a massive chloride conductance in Ort+ neurons. First, histamine dramatically reduced the input resistance of these cells (Fig. 2.3). Moreover, histamine abolished all spontaneous activity, as would be expected from a large decrease in input resistance. Histamine had no effect on the input resistance of control PNs or LNs (Fig. 2.3).

Histamine also affected the membrane potential of Ort+ neurons. The initial resting potential of Ort+ GABA-LNs was -53 ± 1 mV, and these cells were consistently hyperpolarized by histamine, to a new value of -71 ± 2 mV (Fig. 2.4A). PNs had an initial resting potential which was more hyperpolarized than that of GABA-LNs (-64 ± 1 mV), and accordingly the effects of histamine on membrane potential were more modest and varied, with some cells becoming slightly hyperpolarized by histamine, and others becoming slightly depolarized (Fig. 2.4B; see Discussion). On average, histamine caused Ort+ PNs to rest at -65 ± 3 mV (Fig. 2.4B). There was again no significant effect on the membrane potential of control PNs or GABA-LNs (Fig. 2.4A,B).

Figure 2.2: Histamine suppresses stimulus-evoked activity in Ort-expressing neurons.

(A) A cell-attached recording showing spikes in an Ort-expressing antennal lobe PN (left) in a regular saline bath. Subsequent bath application of histamine (100 µM) abolishes both spontaneous and odor-evoked spikes (right). Horizontal bars indicate the period (500 msec) of the odor stimulus. For all sample traces in this figure, the odor was pentyl acetate (10^{-2} dilution).
(B) A whole-cell recording of an Ort-expressing PN. Increasing concentrations of histamine produce greater suppression of activity, and suppression is reversed by wash-out. Note that this particular PN is depolarized by histamine, which we observed in several PNs; others were hyperpolarized or showed no change in resting membrane potential (see Discussion).
(C) Same as above, but in an Ort-expressing antennal lobe GABA-LN.
(D) Odor responses in saline, 100 µM histamine, and after wash-out (measured as the odor-evoked change in membrane potential). Each connected set of circles represents a different PN recording, and bars represent means (n = 8 Ort+ and 5 control). Histamine significantly reduces the odor response in Ort+ flies ($p < 0.001$, paired t-test). In control flies that lack the *UAS-ort* transgene, the odor response before and during histamine application is not significantly different ($p = 0.69$, paired t-test).
(E) Whole-cell recordings from a PN and a GABA-LN that did not express Ort. Histamine had no effect on these cells.

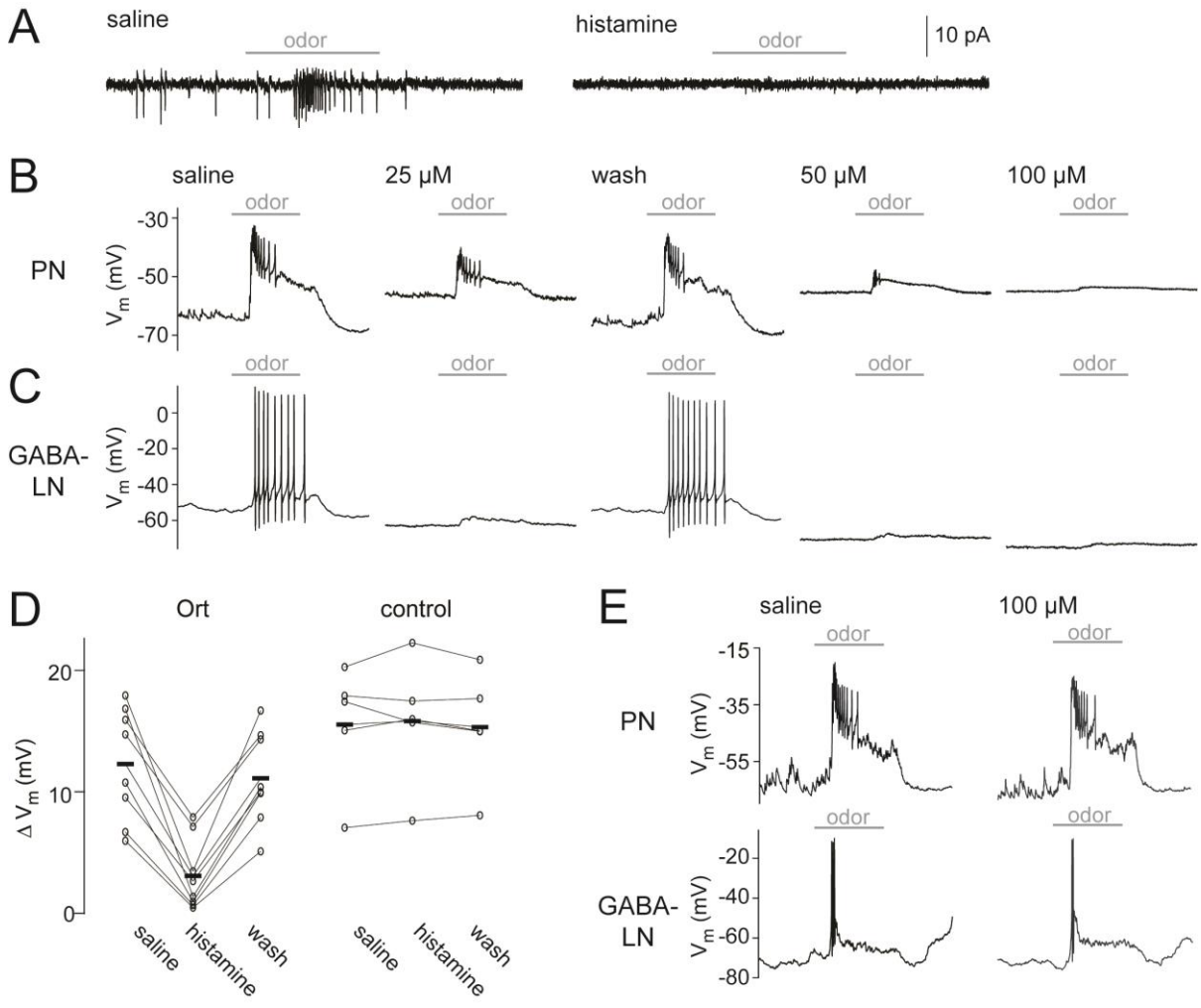

Figure 2.2: Histamine suppresses stimulus-evoked activity in Ort-expressing neurons (continued).

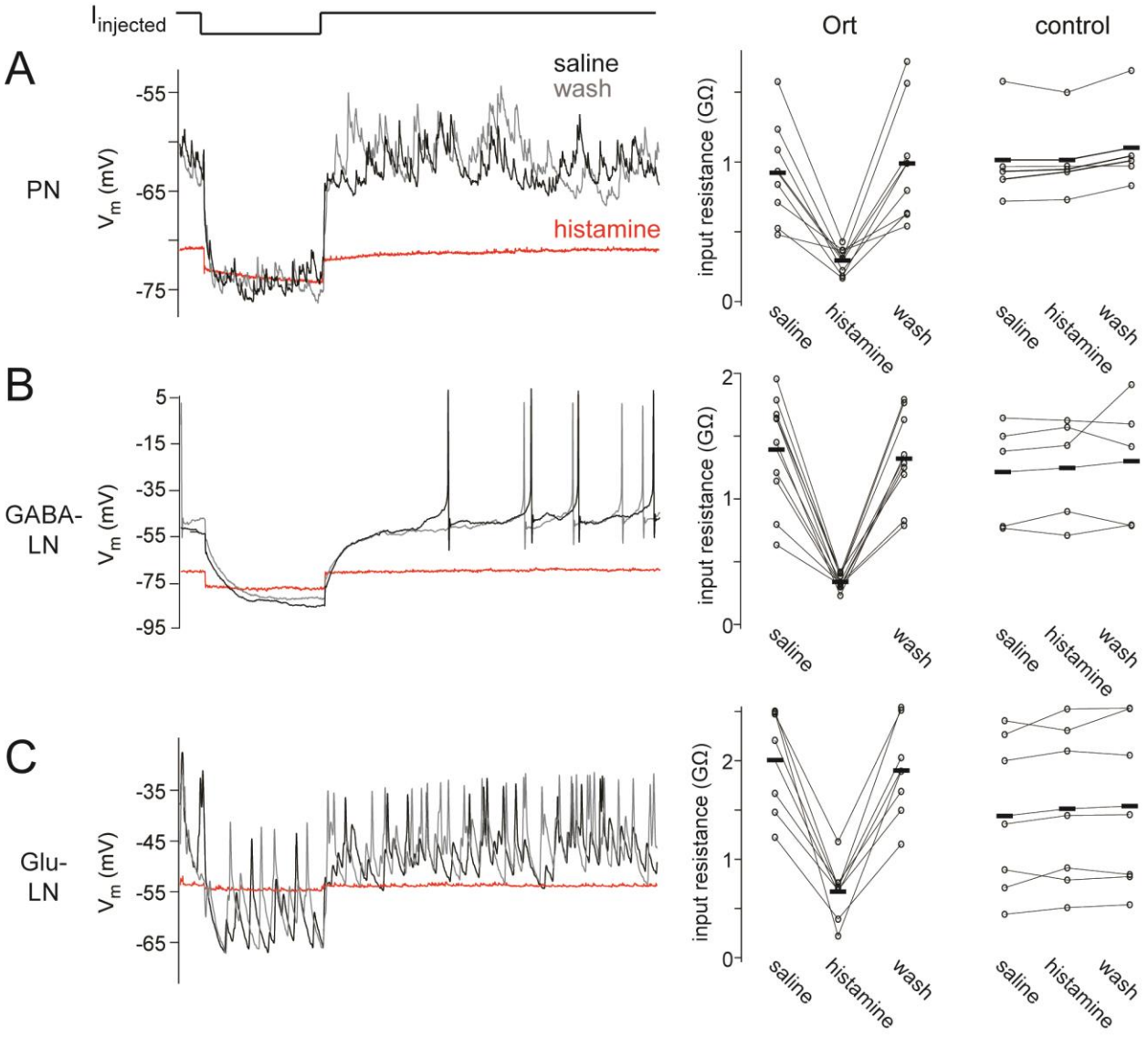

Figure 2.3: Histamine reduces input resistance and suppresses spontaneous activity in Ort-expressing neurons.

(A) A whole-cell recording from an antennal lobe PN showing that histamine (100 µM) reduces input resistance, quantified as the membrane potential change elicited by hyperpolarizing current injection, divided by the magnitude of the current step (500 msec duration). Spontaneous EPSPs are also suppressed by histamine. These effects are reversed upon histamine washout. The plot at right shows the input resistance in histamine, for all PN experiments (n = 8 Ort+ and 5 control).
(B) Same as above, but for a GABA-LNs (n = 10 Ort+ and 5 control).
(C) Same as above, but for a glutamatergic LN (Glu-LN; n = 7 Ort+ and 7 control). In this set of experiments, we used a lower concentration of histamine (25 µM) because this concentration produced near-maximal effects in Glu-LNs. This may reflect a higher level of Gal4 expression in these cells.

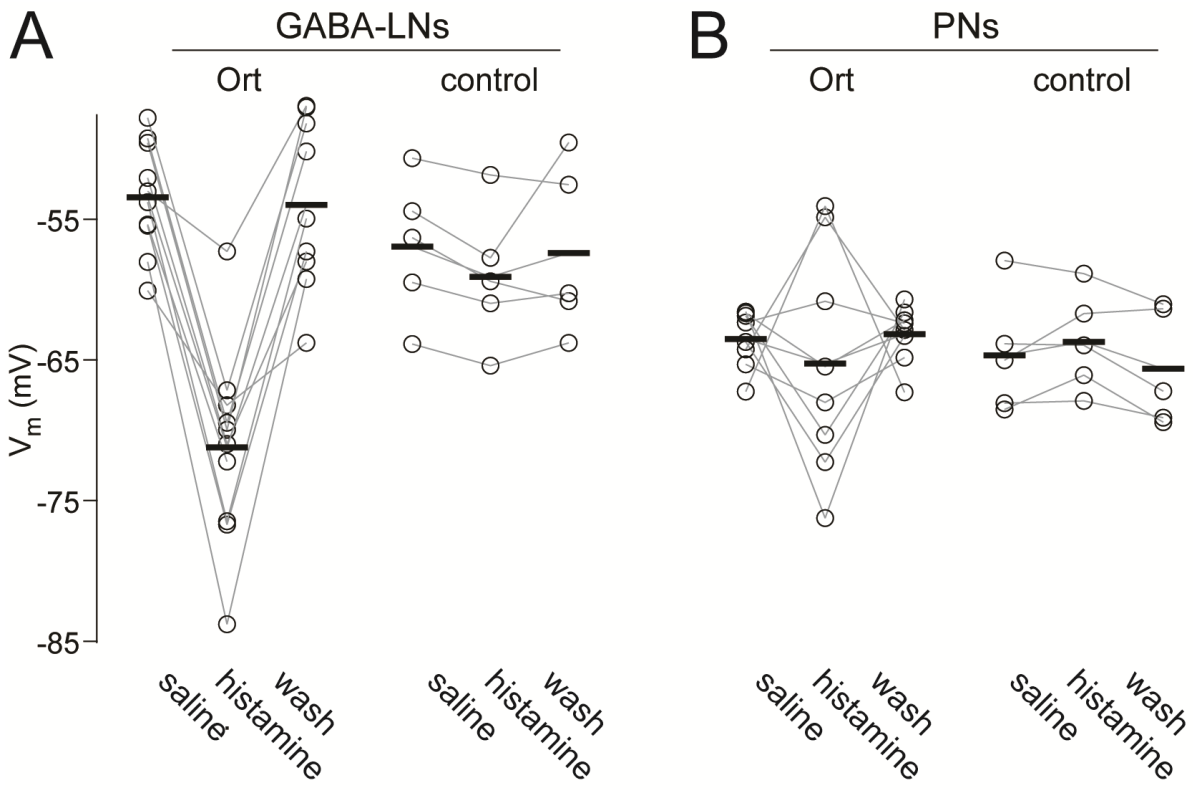

Figure 2.4: Histamine changes the membrane potential of Ort-expressing neurons.

(A) Ort+ GABA-LNs are consistently hyperpolarized by histamine (100 µM). There is no effect on control GABA-LNs (*n* = 10 Ort+ and 5 control). (B) Some Ort+ PNs are hyperpolarized by histamine (100 µM), whereas others are depolarized (*n* = 8 Ort+ and 5 control). Note that the initial resting potential of PNs is more hyperpolarized than that of GABA-LNs.

As one would expect from a small and hydrophilic ligand, the effects of histamine were rapid and reversible. The onset and offset of histamine's effects occurred within the several minutes required for the bath solution to completely equilibrate with the incoming perfusate (Fig. 2.5A-C). The histamine-induced changes in input resistance, membrane potential, and odor responses had similar kinetics, as expected. Prolonged applications of histamine (up to 15 minutes) produced constant effects on all these metrics, without appreciable decay in potency (data not shown).

Finally, we directly compared Ort with the two published alternative techniques designed to transiently silence *Drosophila* neurons, *shibire*^{ts} and halorhodopsin. The *shibire*^{ts} transgene encodes a form of dynamin which misfolds at restrictive temperatures, thereby preventing synaptic vesicle formation (Kitamoto, 2001). Halorhodopsin is a light-activated chloride pump which hyperpolarizes cells (Berni et al., 2012; Inada et al., 2011). The ideal technique for silencing neurons would be both potent (i.e., it would completely silence activity) and selective (it would directly affect only the neurons expressing the effector molecule). To compare the potency and selectivity of Ort with *shibire*^{ts} and halorhodopsin, we employed all three techniques at silencing olfactory receptor neurons (ORNs). We chose ORNs as our targets in these experiments because *shibire*^{ts} affects neurotransmitter release rather than spike initiation, and so its effects are only visible in neurons postsynaptic to the neurons expressing Gal4. In other words, in order to assess the ability of *shibire*^{ts} to silence activity in the antennal lobe, we needed to express Gal4 in neurons presynaptic to the antennal lobe.

We crossed flies expressing each UAS transgene with flies expressing Gal4 in a broad population of ORNs (Sweeney et al., 2007). In each genotype, we recorded from postsynaptic PNs while silencing ORNs. If ORNs were silenced completely, we would expect essentially all

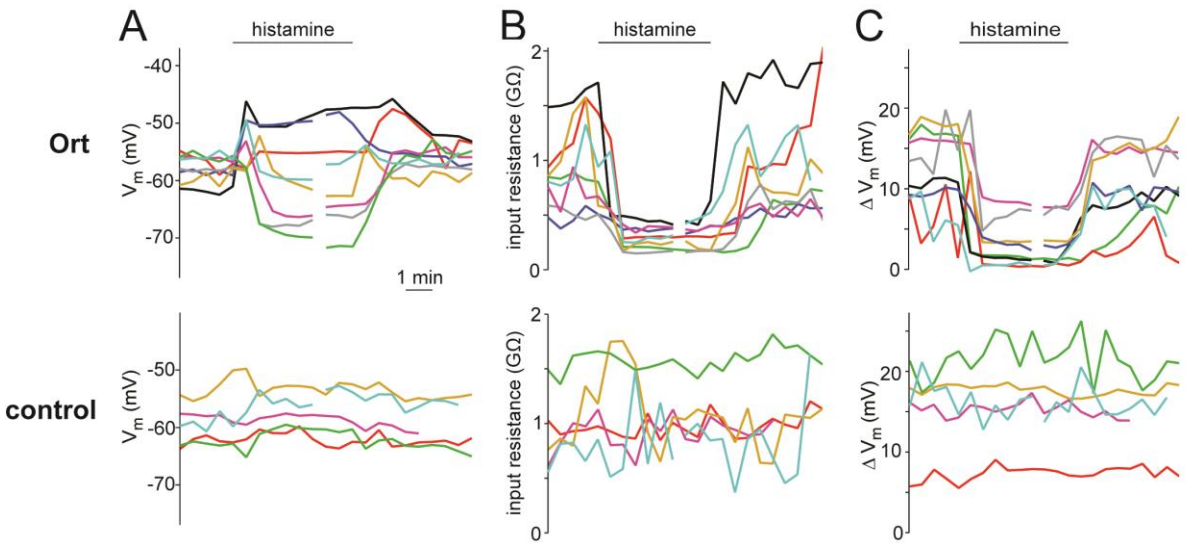

Figure 2.5: Time course of the effect of histamine.

(A) Time course of the effect of histamine (100 µM) on the membrane potential for all recorded Ort+ and control PNs. The bar indicates the period when histamine began to enter and exit the bath. Each trace represents a different PN recording. Broken traces indicate that a period of time is omitted from the display, so that all traces could be aligned at their wash-on and wash-out times. The time base is the same for all panels.
(B) Same as above, but for input resistances.
(C) Same as above, but for odor responses.

spontaneous and odor-evoked activity in PNs to disappear. This is because ORNs are the only major source of excitatory input to PNs, and ORNs normally spike spontaneously, producing excitatory postsynaptic potentials in PNs (Kazama and Wilson, 2008; Kazama and Wilson, 2009). Note that all these techniques likely affect only the ORN axons in the brain, as the ORN somata and dendrites are housed in the antennae and so are likely inaccessible to any of these manipulations. Neurotransmitter release from ORNs should be inhibited by either hyperpolarizing their axons (using Ort or halorhodopsin) or preventing synaptic vesicle formation in axons (with *shibire*^{ts}).

We found that Ort proved effective in silencing ORNs. As one would expect if ORN terminals were clamped at a hyperpolarized potential, we observed that odor-evoked activity in PNs was severely reduced by histamine. On average, the magnitude of PN odor response dropped by 84% (Fig. 2.6A,B). Histamine also eliminated the barrage of spontaneous excitatory postsynaptic potentials in PNs that arises from normal spontaneous ORN spiking (Kazama and Wilson, 2008; Kazama and Wilson, 2009), and as a consequence, PNs were hyperpolarized. Importantly, histamine had little effect in recordings from PNs in control flies (Fig. 2.6B).

By comparison, *shibire*^{ts} was less consistent and specific. In flies where ORNs expressed *shibire*^{ts}, raising the bath to a restrictive temperature (29-30 °C) to inactivate ORNs produced variable effects. On average, the temperature shift reduced PN odor responses by 52% (Fig. 2.6C,D). Spontaneous activity was also reduced. The membrane potential was depolarized by the temperature shift (generally by > 10 mV), and in several experiments the recording was lost. Shifting the bath temperature also depolarized control cells, indicating that this effect was unrelated to *shibire*^{ts}. Moreover, in control cells, the temperature shift reduced PN odor responses by 28% (Fig. 2.6D). Overall, the effect of the temperature shift was still significantly

Figure 2.6: Comparison between Ort, *shibire*^{ts}, and halorhodopsin in silencing ORN input to PNs.

(A) A recording from a PN in a fly where Ort is selectively expressed in ORNs. Horizontal bar indicates the period (500 ms) of odor application. Histamine dramatically reduces odor-evoked activity in the PN, indicating that it is effective in silencing ORNs. Histamine also eliminates spontaneous EPSPs. In this example, the odor is pentyl acetate.
(B) Odor response in regular saline, 100 μM histamine, and wash (measured as the odor-evoked change in membrane potential, $n = 7$ Ort and 9 control genotype). Histamine significantly reduces the odor response in flies where ORNs express Ort ($p < 0.005$, paired *t*-test). In control flies, histamine has little effect, although the small amount of potentiation is in this case statistically significant ($p = 0.02$, paired *t*-test).
(C) A recording from a PN in a fly where *shibire*^{ts} is selectively expressed in ORNs. Shifting the bath to the restrictive temperature inhibits odor-evoked activity in this recording, albeit partially, and eliminates most of the spontaneous activity. The membrane potential also depolarizes. In this example, the odor is a blend of fenchone, pentyl acetate, benzaldehyde, ethyl acetate and ethyl butyrate.
(D) Odor response at the restrictive and permissive temperature ($n = 10$ *shibire*^{ts} and 7 control genotype). Raising the temperature significantly reduces the odor response in *shibire*^{ts} flies ($p < 0.001$, paired *t*-test). Shifting the bath temperature also modestly reduces the odor response of control flies ($p < 0.05$, paired *t*-test).
(E) A recording from a PN in a fly where halorhodopsin is selectively expressed in ORNs. Illuminating the preparation with green light had little effect. Here the odor is trans-2-hexenal.
(F) Odor response in interleaved trials with light versus no light ($n = 9$ halorhodopsin and 6 control genotype). Light does not have a significant effect in either halorhodopsin flies or control flies ($p = 0.26$ and 0.22, paired *t*-tests).
(G) At higher light intensities than those used above (E,F), we saw that light produced a nonspecific suppression of activity. This example PN was recorded in a fly where the Gal4 transgene was omitted, so no halorhodopsin should be expressed. The magnitude of this effect was similar in flies with and without the transgene. The light intensity here was four times that used in (E,F); see Experimental Procedures.

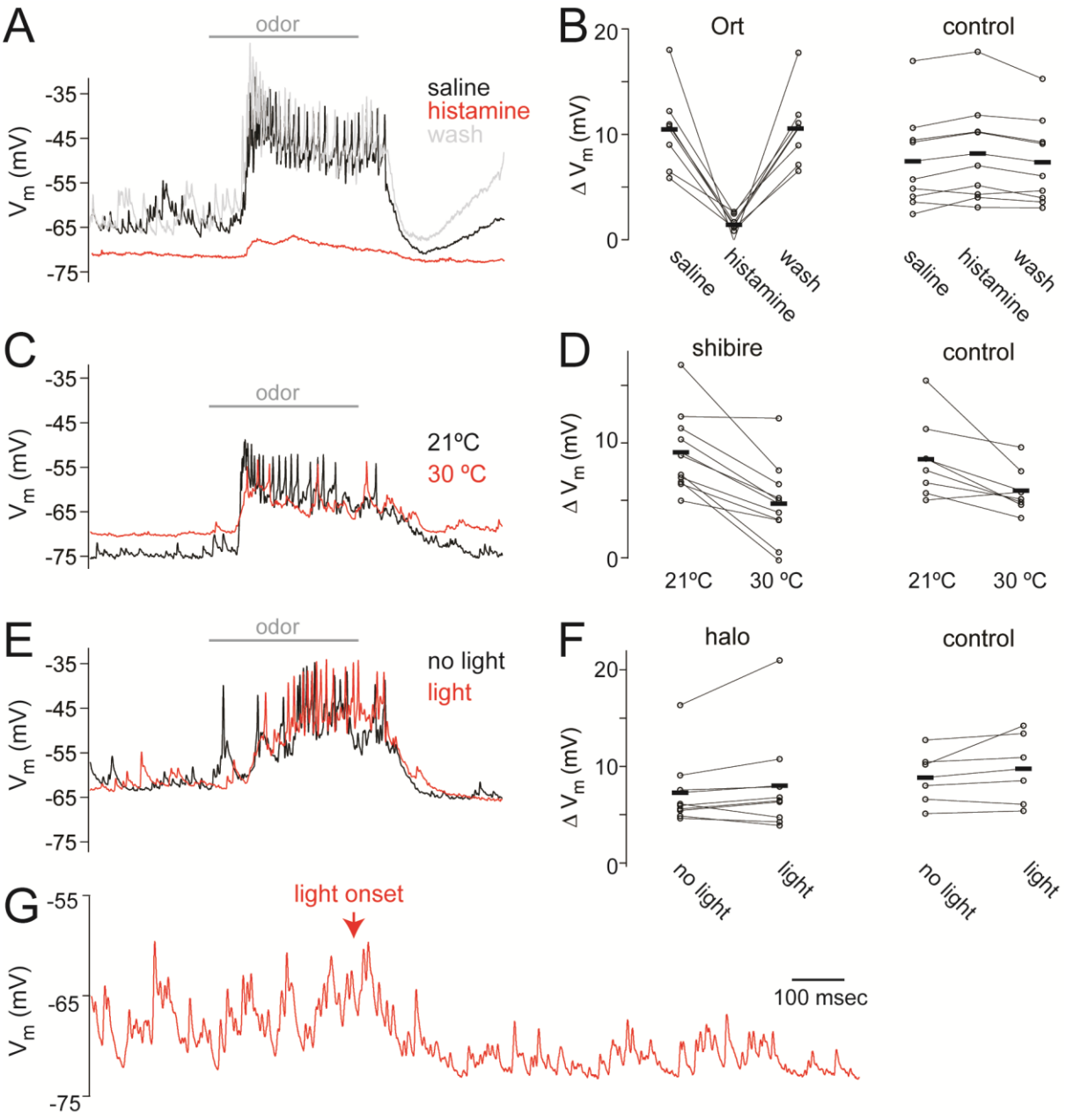

Figure 2.6: Comparison between Ort, shibirets, and halorhodopsin in silencing ORN input to PNs (continued).

different in control and *shibire*^{ts} flies, indicating that *shibire*^{ts} was acting as intended, but the nonspecific effects of the temperature shift were sizeable.

Halorhodopsin was the least effective technique in this experimental context. In flies where ORNs expressed halorhodopsin, illuminating the brain produced no significant change at light intensities that were low enough to avoid nonspecific effects (Fig. 2.6E,F). In our pilot experiments, we found that higher light intensities strongly hyperpolarized PNs in control flies (i.e., flies that lacked the *UAS-halorhodopsin* transgene; Fig. 2.6G).

Discussion

In mammalian systems, several techniques have been developed in recent years for transiently inactivating neurons using non-native neurotransmitter receptor (Lechner et al., 2002; Lerchner et al., 2007; Magnus et al., 2011; Slimko et al., 2002; Wulff et al., 2007). The goal in using a non-native receptor is to avoid activation by endogenous ligands. Here, we took a different approach: we exploited the fact that histamine is present only sparsely in the nervous system outside of the eye, where it is the native neurotransmitter of photoreceptors (Hardie, 1989). Indeed, there are only about 20 histaminergic neurons outside of the optic lobes, and many brain regions are devoid of histaminergic processes. These areas include the antennal lobe, mushroom bodies, and the central complex ((Nassel, 1999; Pollack and Hofbauer, 1991) and Fig. 2.1). In these brain regions, histamine can potentially be used as an artificial neurotransmitter, because it is not normally used as a neurotransmitter. Using a receptor which is native to *Drosophila* is convenient for achieving high levels of surface expression without further transgene optimization. Moreover, Ort is an excellent candidate for a transgenic effector molecule because it forms homomeric channels – thereby avoiding the need for multiple transgenes – and because the Ort channel has a large conductance and shows little desensitization

(Pantazis et al., 2008). Importantly, Ort channels are highly selective for histamine over GABA (Zheng et al., 2002). These properties motivated our investigation of Ort as a candidate effector molecule.

We found that the histamine/Ort system can be a potent and selective method for neural inactivation. It can produce essentially complete inactivation, and its effects are similar in diverse cell types, under the control of various Gal4 drivers. This is important because it shows that the technique is robust to the properties of the Gal4 driver used to control transgene expression. Moreover, the effects of histamine are completely reversible.

How does the histamine/Ort system actually work? Ort is a chloride channel, and the nominal chloride reversal potential in these experiments was -121 mV, given the compositions of the external and pipette solutions. One might therefore expect histamine to dramatically hyperpolarize Ort+ neurons. This is not what we observed. Histamine did clearly open a massive conductance – more than doubling the resting conductance –but it generally produced a modest hyperpolarization, and some cells were even modestly depolarized. In a typical cell, histamine clamped the membrane potential between -60 and -75 mV. This suggests that opening Ort channels causes a large amount of chloride to enter the cell, thereby depolarizing the chloride reversal potential. In other words, the chloride gradient partially collapses. Strong activation of ligand-gated chloride channels is known to be capable of partially collapsing chloride gradients in mammalian neurons (Staley et al., 1995). When a ligand-gated invertebrate chloride channel is misexpressed in mammalian neurons, application of its ligand produces effects on the membrane potential which are similar to what we observe here (Slimko et al., 2002). In sum, these techniques appear to work largely by shunting inhibition, rather than hyperpolarizing inhibition.

The motivation for these experiments arose from the limitations of currently available techniques intended to produce transient neural inactivation in *Drosophila*. The *shibire*^{ts} technique has been very widely used, but its limitations are also well-known (Luo et al., 2008; Simpson, 2009). First, temperature changes alter virtually every aspect of a fly's physiology, which can make it difficult to interpret negative controls. Second, in order to verify that this technique has inactivated a neuron, one cannot record from that neuron itself; rather, one would need to record postsynaptic to that neuron. Third, the mis-folded dynamin will only inhibit synaptic vesicle recycling if it is present in high copy number, and so this technique relies on achieving high transgene expression levels (Kitamoto, 2002). Fourth, this technique should not affect release of peptidergic vesicles, which do not depend on rapid endocytotic recycling. Finally, because dynamin has multiple functions within cells, overexpressing this transgene can cause necrosis, even at permissive temperatures (Gonzalez-Bellido et al., 2009).

Similarly, there are also limitations associated with the current generation of optogenetic reagents for hyperpolarizing neurons. These reagents are light-activated microbial chloride or proton pumps which should generate an outward pump current which hyperpolarizes neurons (Fenno et al., 2011). However, these pumps have a relatively low single-molecule conductance, meaning that they must be expressed at high levels, and they must also be trafficked efficiently to the cell membrane, which has been difficult to achieve (Fenno et al., 2011), particularly in *Drosophila* (Venken et al., 2011). Recently, halorhodopsin has been found to be effective at inactivating neurons in the *Drosophila* larva *in vivo* (Berni et al., 2012; Inada et al., 2011), demonstrating that it can be useful in experimental contexts different from those of our study. The differential efficacy of halorhodopsin in those cases and in our case may reflect differences in the cell types, Gal4 drivers, or other methodological differences.

The immediate application for which we developed this technique is to inactivate specific neurons with histamine, while simultaneously recording from other neurons *in vivo*. In this way, one can study how circuit physiology is affected by silencing specific neurons within the circuit. Several studies have transiently activated specific neurons in this experimental configuration (Huang et al., 2010; Pulver et al., 2009; Yaksi and Wilson, 2010; Yao et al., 2012); what has been lacking is a robust and highly-selective method of transient inactivation.

This technique does have limitations. First, it cannot be used in a *Drosophila* brain region where histamine has major endogenous effects, such as the visual system. Several regions of the central nervous system receive sparse histaminergic innervation, including much of the lateral and dorsal protocerebrum (Fig. 2.1), but it is not known whether histamine has major endogenous effects in these regions. A necessary and sufficient control for endogenous effects will be to compare flies with and without Ort misexpression.

Second, this technique requires delivery of exogenous histamine, and so cannot be used in intact flies. In principle, this might be circumvented by injecting caged histamine, and then illuminating the intact fly to photo-uncage the ligand. A similar approach has been used previously to transiently activate specific neurons *in vivo*, in that case using caged ATP and transgenic expression of purinergic receptors (Lima and Miesenbock, 2005).

Ultimately, the desired properties of a genetic effector system depend on the experimental setting (Luo et al., 2008; Simpson, 2009; Thum et al., 2006). For this reason, it is useful to develop multiple complementary systems. Recent years have seen new techniques to monitor neural activity *in vivo* in *Drosophila*, as well new reagents for selectively expressing transgenes in specific neurons (Simpson, 2009; Venken et al., 2011). The Ort/histamine system

is a promising component of this toolkit for probing functional connectivity between identified neurons *in vivo*.

Experimental Procedures

Fly stocks

Flies were raised on standard cornmeal agar medium supplemented with rehydrated potato flakes on a 12 h light/dark cycle at 25°C. The two exceptions were flies expressing *UAS-shibire^{ts}*, which were raised at 18°C, and flies expressing halorhodopsin, which were raised in the dark on food supplemented with all-trans retinal. All-trans retinal was prepared as a 35mM stock solution in ethanol and diluted 10-fold in water before mixing with rehydrated potato flakes; this mix was layered on top of conventional food. All experiments were performed on adult female flies 1-3 days post eclosion, except for the experiments with *shibire^{ts}*, where some flies were male. The genotypes used were as follows:

Fig. 2.2A,B – *GH146-Gal4,UAS-CD8:GFP/UAS-ort*
Figs. 2.2C,2.4C – *UAS-ort/UAS-CD8:GFP;NP3056-Gal4/+*
Fig. 2.2D,2.3A,2.4B,2.5 – *GH146-Gal4,UAS-CD8:GFP/+* (control) and *GH146-Gal4,UAS-CD8:GFP/UAS-ort* (Ort)
Fig. 2.2E – *GH146-Gal4,UAS-CD8:GFP/ +* (PN) and *UAS-CD8:GFP/+;NP3056-Gal4/+* (LN)
Figs. 2.3B,2.4A – *UAS-CD8:GFP/+;NP3056-Gal4/+* (control) and *UAS-ort/UAS-CD8:GFP;NP3056-Gal4/+* (Ort)
Fig. 2.3C – *OK371-Gal4,UAS-CD8:GFP/+* (control) and *OK371-Gal4,UAS-CD8:GFP/UAS-ort* (Ort)
Fig. 2.6A – *pebbled-Gal4/+;UAS-ort/+*
Fig. 2.6B – *pebbled-Gal4/+* and *UAS-ort/+* (control) and *pebbled-Gal4/+;UAS-ort/+* (Ort)
Fig. 2.6C – *pebbled-Gal4/+;;UAS-UAS-shibire^{ts}/+*
Fig. 2.6D – *pebbled-Gal4* (control) and *pebbled-Gal4/+;;UAS-shibire^{ts}/+* (*shi^{ts}*)
Fig. 2.6E – *pebbled-Gal4/+;UAS-eNpHR-50C/+;UAS-eNpHR-19C,UAS-eNpHR-34B/+*;
Fig. 2.6F – *UAS-eNpHR-50C;UAS-eNpHR-19C,UAS-eNpHR-34B* (control) and *pebbled-Gal4/+;UAS-eNpHR-50C/+;UAS-eNpHR-19C,UAS-eNpHR-34B/+* (halo)

Fig. 2.6G – *UAS-eNpHR-50C;UAS-eNpHR-19C,UAS-eNpHR-34B*

Fly stocks were previously published as follows: *GH146-Gal4* (chromosome II) (Stocker et al., 1997), *NP3056-Gal4* (chromosome III) (Chou et al., 2010a), *OK371-Gal4* (chromosome II) (Mahr and Aberle, 2006), *UAS-CD8:GFP* (chromosome II or III) (Lee and Luo, 1999), *UAS-ort* (chromosome II) (Rister et al., 2007), *UAS-eNpHR-50C;UAS-eNpHR-19C,UAS-eNpHR-34B* (chromosomes II and III) (Inada et al., 2011), *UAS-shibire^{ts}* (chromosome III) (Kitamoto, 2001), *pebbled-Gal4* (X chromosome) (Sweeney et al., 2007). Stocks of *OK371-Gal4* and *UAS-CD8:GFP* were obtained from the Bloomington Drosophila Stock Center.

Electrophysiological Recordings

In vivo whole-cell patch clamp recordings were performed as previously described (Wilson and Laurent, 2005a; Wilson et al., 2004). In this preparation, the antennae and maxillary palps of the fly remained dry and accessible to odors, while the brain was bathed in saline and was accessible to patch-clamp electrodes. The saline contained (in mM): 103 NaCl, 3 KCl, 5 N-tris(hydroxymethyl) methyl-2-aminoethane-sulfonic acid, 8 trehalose, 10 glucose, 26 $NaHCO_3$, 1 NaH_2PO_4, 1.5 $CaCl_2$, and 4 $MgCl_2$ (osmolarity adjusted to 270-275 mOsm). The saline was bubbled with 95% O_2/ 5% CO_2 to a pH of 7.3, and was flowed continuously over the preparation at a rate of 2 mL/min. Patch pipettes were filled with a solution containing the following (in mM): 140 potassium aspartate, 10 HEPES, 1 EGTA, 4 MgATP, 0.5 Na_3GTP, 1 KCl, and 13 biocytin hydrazide. The pH of the internal solution was adjusted to 7.2 and the osmolarity was adjusted to ~265 mOsm. Recordings were performed with an Axopatch 200B amplifier (Axon Instruments). Voltages were low-pass filtered at 5 kHz and digitized at 10 kHz. Voltages were corrected for the measured liquid junction potential of +13 mV, which was subtracted from recorded voltages post hoc (Gouwens and Wilson, 2009). Series resistance was uncompensated. To record from PNs, GABA-LNs and Glu-LNs (in Fig. 2.2-5), we targeted our electrodes to cells labeled with

GFP. To record from unlabeled PNs (in Fig. 2.6), we targeted our electrodes to the cluster of PN cell bodies immediately anterodorsal to the antennal lobe neuropil, and we confirmed that all these cells had small-amplitude action potentials (<12 mV), which is characteristic of PNs (Wilson et al., 2004). In these types of whole-cell recordings, the seal conductance is large enough (relative to the high input resistance of these cells) to produce a discernible depolarization in the resting potential; for this reason, we injected a small amount of constant hyperpolarizing current in order to bring the cell back down to its native resting potential (Gouwens and Wilson, 2009). The native resting potential of PNs and GABA-LNs was estimated by measuring spontaneous spiking in cell-attached mode prior to rupturing the seal, and then injecting enough constant hyperpolarizing current to match the spontaneous spike rate in whole-cell mode. Both Ort+ PNs and control PNs had seal resistances of >1GΩ prior to rupturing the seal. Because spontaneous spikes are typically not visible in cell-attached recordings from Glu-LNs, we are less confident about the native resting potential of these cells, and we did not inject any holding current into these cells. Cell-attached recordings were performed in voltage-clamp mode, and the command potential was adjusted so that no current was passed through the electrode. In these recordings, the patch pipettes were filled with external saline, and data was low-passed filtered at 1kHz. Histamine or histamine dihydrochloride was prepared as a 100 mM stock solution in water, and the stock was added to the reservoir feeding the bath flowing over the brain to achieve the desired final concentration. The stock solution was prepared fresh every week. For experiments using shibire^{ts}, the saline perfusate was heated from room temperature (~21 °C) to 29-30° C over a period of ~5 min using a TC-324B temperature controller equipped with an in-line solution heater (Warner Instruments). The temperature of the bath was monitored continuously with a submerged thermistor.

Odor stimulation

Odors used were diluted 100-fold in paraffin oil (except for pentanoic acid, which was diluted 10,000-fold, and pentyl acetate, which was diluted 1,000-fold in some experiments) and delivered via a custom-built olfactometer, which further dilutes the headspace of the odor vial 10-fold in air (Olsen et al., 2007). Odorized air was delivered to the head of the fly at a flow rate of 2.2 mL/min. Odor stimuli were applied for 500-msec every 30 sec, with 5-10 trials per stimulus. Because we did not know in advance of obtaining a recording what odor(s) a cell might respond to, we prepared a small panel of odors that collectively are effective at stimulating many antennal lobe neurons (pentyl acetate, methyl salicylate, trans-2-hexenal, pentanoic acid, and also a blend of fenchone, pentyl acetate, benzaldehyde, ethyl acetate and ethyl butyrate). Once we obtained a recording, we tried odors from this set until we found an effective stimulus. If no response could be obtained with any of these stimuli, we discarded the cell.

Optogenetic stimulation

Light was delivered via a 100-W Hg arc lamp (Olympus) attenuated with a ND-25 neutral-density filter, band-pass filtered at 540–580 nm, and delivered to the specimen through the 40× water-immersion objective used to visualize the preparation for patch-clamp recording. The light intensity at the specimen was measured as 8.5 mW/mm^2 using an optical power meter (Newport 1916-C) with a photodetector (818P-015-19, intensity reported at 560 nm) positioned behind a pinhole aperture. We chose this light intensity because it was the highest intensity that did not produce a nonspecific effect of light (see Fig. 2.6G for an example of a nonspecific effect at 37 mW/mm^2). Pulses of light (2 sec in duration, beginning 1 sec before odor onset) were controlled with a shutter (Uniblitz) controlled by a TTL pulse. Odor presentations with and without light were interleaved, with a total of 12-20 presentations per odor per experiment.

Histochemistry

Histamine immunostaining (Fig. 2.1) we followed a modified version of previously published procedures (Panula et al., 1988; Pollack and Hofbauer, 1991). Briefly, the brain and ventral nerve cord were dissected out and fixed in 4% 1-ethyl-3-(3-dimethylaminopropyl) carbodiimide in PBS for 5 hours at 4° C. Samples were rinsed with PBS, and incubated in blocking solution (5% normal goat serum [Vector Laboratories] in PBST [0.2% Triton X-100 in PBS]) for 30 min, and then incubated in 1:500 rabbit anti-histamine antibody (Abcam ab43870) and 1:50 mouse nc82 antibody (Developmental Studies Hybridoma Bank) in blocking solution at 4°C for 2 d. After washing for 20 min in PBST, samples were incubated with 1:250 goat anti-rabbit:Alexa Fluor 488 and 1:250 goat anti-mouse:Alexa Fluor 633 (Invitrogen) in blocking solution at room temperature for 1 d. Samples were then mounted in Vectashield (Vector Laboratories) and imaged with a laser-scanning confocal microscope (Zeiss LSM 510).

Data analysis

The odor-evoked membrane potential response was computed by low-pass filtering the membrane potential at 10 Hz (to remove spikes), and then taking the mean across trials over the 500-msec odor stimulus period, minus the mean in the period just before the odor stimulus. Input resistance was computed as the membrane potential change elicited by a step of negative current injected into the soma, divided by the magnitude of the current step. Group data in the text is reported as mean ± SEM, computed across experiments.

Acknowledgements

We thank Chi-Hon Lee for *UAS-ort* flies, Toshi Kitamoto for *UAS-shibire*^{ts} flies, Akinao Nose for *UAS-eNpHR* flies, John Tuthill for performing ventral nerve cord dissections, and Pertti Panula for advice on histamine immunohistochemistry. This work was supported by a research

project grant from the National Institutes of Health (R01DC008174). W.W.L. is supported by an HHMI International Research Fellowship and a Presidential Scholarship from the MD-PhD Program at Harvard Medical School. R.I.W. is an HHMI Early Career Scientist.

CHAPTER 3:

Glutamate is an inhibitory neurotransmitter in the *Drosophila* olfactory system

---

The work in this chapter has been published as:

W.W. Liu & R.I. Wilson (2013) Glutamate is an inhibitory neurotransmitter in the *Drosophila* olfactory system. *Proceedings of the National Academy of Sciences* 110:10294-9.

I performed the experiments and analyzed the data. Both I and R.I.W. designed the experiments and wrote the paper.

Summary

Glutamatergic neurons are abundant in the *Drosophila* central nervous system, but their physiological effects are largely unknown. In this study, we investigated the effects of glutamate in the *Drosophila* antennal lobe, the first relay in the olfactory system and a model circuit for understanding olfactory processing. In the antennal lobe, one third of local neurons are glutamatergic. Using *in vivo* whole-cell patch clamp recordings, we found that many glutamatergic local neurons (Glu-LNs) are broadly tuned to odors. Iontophoresed glutamate hyperpolarizes all major cell types in the antennal lobe, and this effect is blocked by picrotoxin or by transgenic RNAi-mediated knockdown of the *GluClα* gene, which encodes a glutamate-gated chloride channel. Moreover, antennal lobe neurons are inhibited by selective activation of Glu-LNs using a non-native genetically-encoded cation channel. Finally, transgenic knockdown of *GluClα* in principal neurons disinhibits the odor responses of these neurons. Thus, glutamate acts as an inhibitory neurotransmitter in the antennal lobe, broadly similar to the role of GABA in this circuit. However, because glutamate release is concentrated between glomeruli, whereas

GABA release is concentrated within glomeruli, these neurotransmitters may act on different spatial and temporal scales. Thus, the existence of two parallel inhibitory transmitter systems may increase the range and flexibility of synaptic inhibition.

Introduction

Identifying the physiological effects of neurotransmitters is critical to deciphering neural circuit function. In the vertebrate central nervous system (CNS), glutamate serves as the major excitatory neurotransmitter, while GABA and glycine serve as the major inhibitory neurotransmitters. Like the vertebrate CNS, the *Drosophila* CNS uses several major neurotransmitters. Among these, acetylcholine is the major fast excitatory neurotransmitter, and GABA is the major fast inhibitory neurotransmitter. Recent studies have demonstrated that glutamatergic neurons are widespread in the *Drosophila* CNS (Daniels et al., 2008; Raghu and Borst, 2011), but its effects in the CNS are poorly understood. Much attention has been focused on the idea that the effects of glutamate in the *Drosophila* CNS are excitatory (Das et al., 2011a; Das et al., 2011b; Miyashita et al., 2012; Sudhakaran et al., 2012; Wu et al., 2007; Xia et al., 2005). However, this idea has remained largely untested. There are 30 putative ionotropic glutamate receptor subunits in the *Drosophila* genome. Most are homologous to mammalian AMPA/kainate and NMDA receptors (Littleton and Ganetzky, 2000), but the genome also contains a metabotropic glutamate receptor (Parmentier et al., 1996) and a glutamate-gated chloride channel (Cully et al., 1996). This means that glutamate can have a variety of possible physiological effects.

Much of what we know about synaptic physiology in the *Drosophila* CNS comes from studies of the antennal lobe. The antennal lobe is one of the most well-studied regions of the fly brain, and because it bears some homology to the vertebrate olfactory bulb, it has been a model

for understanding olfactory processing (Masse et al., 2009; Wilson, 2011). Roughly one-third of antennal lobe local neurons (LNs) are immunopositive for the vesicular glutamate transporter (60-70 out of ~200 total LNs); these cells are also immunonegative for GABA, unlike most LNs (Chou et al., 2010a; Das et al., 2011a). This implies a major role for glutamate in this neural circuit. There is evidence for several glutamate receptors in the antennal lobe, including NMDA receptors (Das et al., 2011b; Sudhakaran et al., 2012; Xia et al., 2005) and metabotropic glutamate receptors (Devaud et al., 2008; Ramaekers et al., 2001). Knocking down NMDA receptor expression specifically in antennal lobe projection neurons interferes with olfactory habituation (Das et al., 2011b; Sudhakaran et al., 2012). However, the effects of glutamate have not been characterized in this circuit. In this study, we investigated the effect of glutamate on antennal lobe neurons, and also the functional role of glutamatergic neurons in olfactory processing.

Results

Glutamate release is concentrated in the inter-glomerular space

The antennal lobe is divided into ~50 glomeruli (Fig. 3.1A), with each glomerulus corresponding to a different type of olfactory receptor neuron (ORN). Antennal lobe LNs interconnect glomeruli via dendro-dendritic synapses onto projection neurons (PNs), and/or dendro-axonic synapses onto ORNs. Previous studies have shown that some antennal lobe LNs are immunopositive for the vesicular glutamate transporter (VGlut) and immunonegative for GABA (Chou et al., 2010a; Das et al., 2011a). These neurons have somata that are ventral to the antennal lobe, and are labeled by the *OK371-Gal4* line (Fig. 3.1B,C).

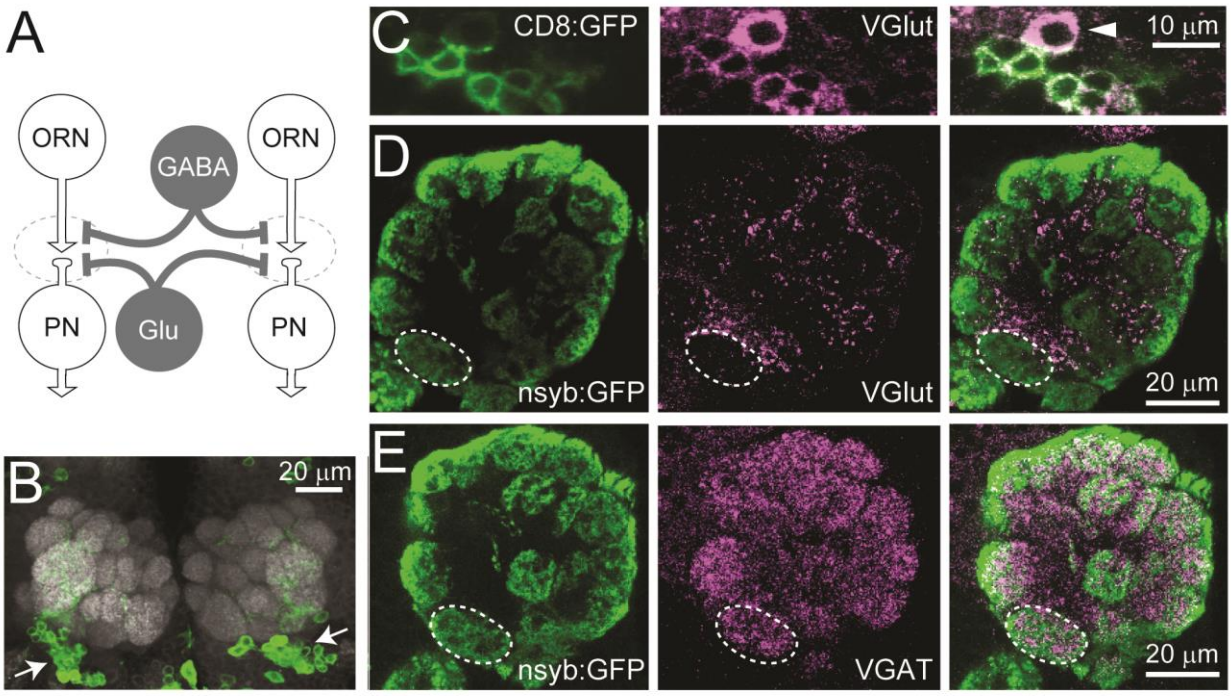

Figure 3.1: Glutamatergic LNs in the antennal lobe.

(A) Schematic of the antennal lobe circuit. Excitatory neurons are in white, and LNs are in gray. Dashed lines encircle glomeruli. Some cell types and connections are omitted for clarity.
(B) Confocal immunofluorescence image of the *Drosophila* brain. Neuropil is labeled with nc82 antibody (white), and cells that express Gal4 under the control of *OK371-Gal4* are labeled with CD8:GFP (green). The somata of Glu-LNs are clustered ventral to the antennal lobes (arrows). Image is a *z*-projection of coronal optical slices through a 27-μm depth.
(C) GFP+ neurons are immunopositive for VGluT (see also Das et al., 2011a). Image is a single 1-μm confocal slice through one of the clusters of Glu-LN somata shown in B. Note that some VGluT+ somata are not GFP+ (arrowhead).
(D) Coronal optical section through one antennal lobe, with glomerular compartments indicated by a presynaptic marker (nsyb:GFP) expressed specifically in ORNs. Note that VGlut is concentrated in the spaces between glomeruli. One glomerulus (VM4, dashed lines) is outlined as a landmark.
(E) Same as D but with staining for the vesicular GABA transporter (VGAT). Note that VGAT immunofluorescence present within each glomerular volume.

In the neuropil, we noticed that VGlut is concentrated primarily in the spaces between glomeruli, and is only sparsely present inside glomeruli (Fig. 3.1D). This contrasts with the vesicular GABA transporter, which is densely and fairly uniformly expressed throughout the antennal lobe neuropil (Fig. 3.1E). This suggests that glutamate and GABA act differently within the antennal lobe.

Glutamatergic LNs have diverse morphologies and odor responses

Next, we performed *in vivo* whole-cell recordings to characterize the physiology of glutamatergic LNs (Glu-LNs), and to examine their morphology. We used GFP to target our electrodes to Glu-LNs, and we filled cells with biocytin via the patch pipette. We observed that these neurons have diverse morphologies, consistent with previous reports (Chou et al., 2010a; Das et al., 2011a), and also diverse physiological properties.

One morphological class of Glu-LNs innervated many glomeruli (Fig. 3.2A). As expected from their morphology, these neurons were broadly tuned to odors (Fig. 3.2B,C). A second class of Glu-LNs had more selective innervation patterns, generally projecting to one ventral glomerulus (Fig. 3.2D). Some of the ORNs innervating this region are narrowly tuned to organic acids (Silbering et al., 2011). Accordingly, some Glu-LNs with this innervation pattern responded preferentially to the organic acid in our test set (butyric acid), although most were broadly tuned (Fig. 3.2E,F). A third class of Glu-LNs sent only sparse projections to olfactory glomeruli, and instead densely innervated the region just posterior to olfactory glomeruli (Fig. 3.2G). This region contains several glomeruli (termed VP1-3) which receive input from hygrosensitive and thermosensitive neurons in the arista (Stocker et al., 1990b). These Glu-LNs typically responded more strongly to water vapor than to odors (Fig. 3.2H,I).

Figure 3.2: Morphology and physiology of Glu-LNs.

(A) Morphology of a Glu-LN, shown as a *z*-projection of a traced biocytin fill. This neuron innervated many olfactory glomeruli, and this pattern was seen in 11 of 29 filled cells. Note innervation of both antennal lobes (black circles), which is typical of Glu-LNs.
(B) A whole-cell current clamp recording from a Glu-LN with this innervation pattern. The spikes fired by this cell (arrow) are small.
(C) Mean stimulus responses of all the Glu-LNs with this innervation pattern (± SEM across experiments), quantified as the change in membrane potential averaged over the stimulus period. Odors are 1: butyric acid, 2: pentyl acetate (high concentration), 3: pentyl acetate (low concentration), 4: water, 5: methyl benzoate, 6: 1-butanol, 7: ethyl acetate.
(D) This neuron innervated mainly a single ventral olfactory glomerulus on both sides of the brain. A similar type of pattern was seen in 8 of 29 fills.
(E) A recording from a neuron with this innervation pattern. Spikes (arrow) are particularly small.
(F) Mean stimulus responses for all the Glu-LNs that mainly innervated one ventral glomerulus.
(G) This neuron innervated the putative hygrosensitive/thermosensitive glomeruli just posterior to the antennal lobe. A similar pattern was seen in 10 of 29 fills.
(H) A recording from a neuron with this innervation pattern. Note prominent spikes (arrow) and large excitatory postsynaptic potentials (arrowhead).
(I) Mean stimulus responses for all the Glu-LNs with this morphology.

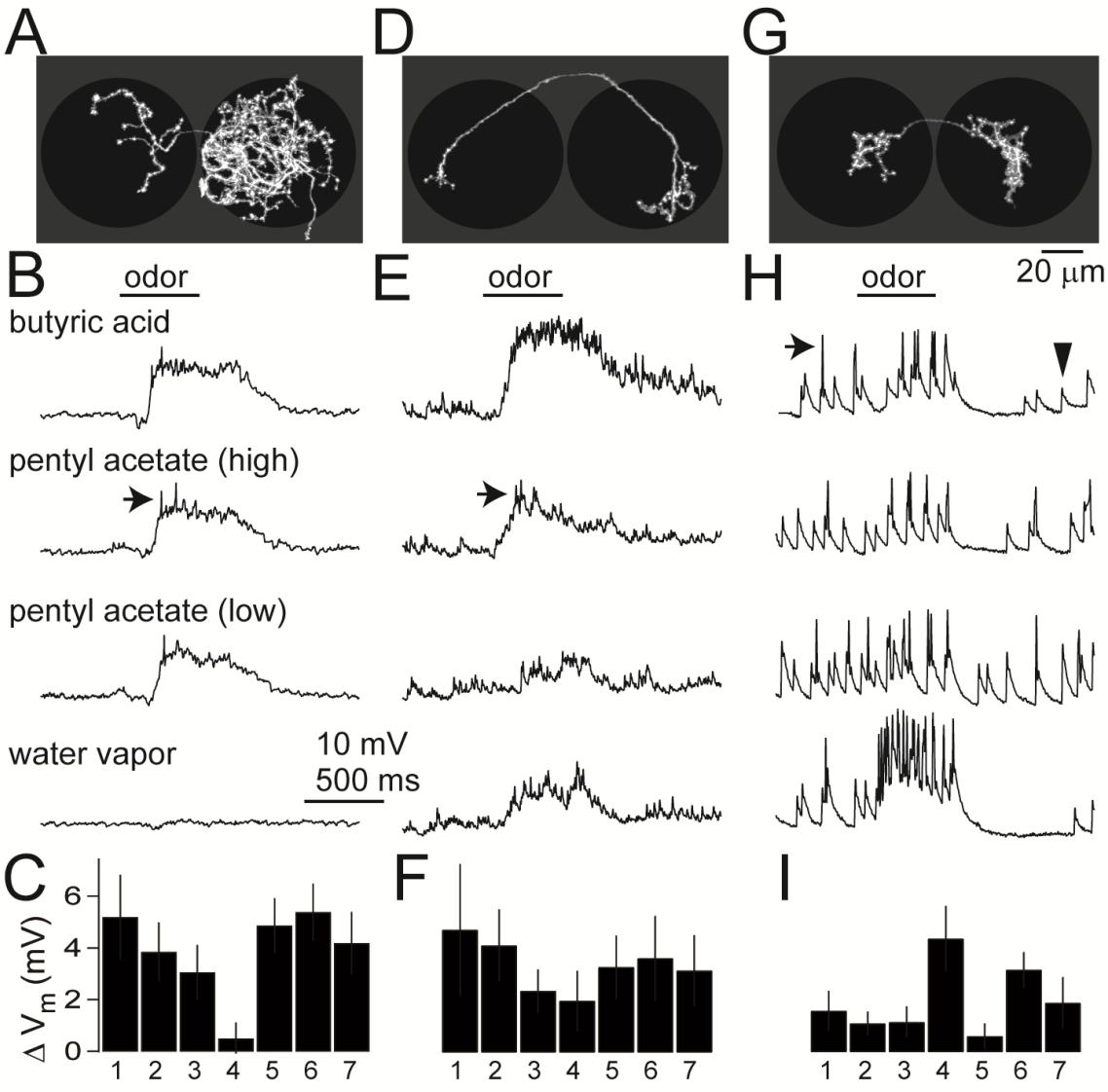

Figure 3.2: Morphology and physiology of Glu-LNs (continued).

These data indicate that Glu-LNs constitute a diverse population of neurons. Nonetheless, most Glu-LNs are broadly tuned, and so most volatile stimuli will recruit many Glu-LNs. This raises the issue of how glutamate affects other neurons in the antennal lobe.

Glutamate hyperpolarizes PNs and GABAergic LNs via a glutamate-gated chloride channel

Next, we asked how exogenous glutamate affects antennal lobe neurons. We performed *in vivo* whole cell recordings from the somata of PNs and GABAergic local neurons (GABA-LNs), using microiontophoresis to apply brief pulses of glutamate into the antennal lobe neuropil. Glutamate consistently hyperpolarized both PNs and GABA-LNs (Fig. 3.3A).

Most of the glutamate response was blocked by bath-applied picrotoxin (100 μM), and the effect of picrotoxin was similar in PNs and GABA-LNs (Fig. 3.3A,C). Picrotoxin is a broad-spectrum chloride channel pore blocker, and although it is most commonly used as a $GABA_A$ antagonist, it can also block GluCl homomers (Cleland, 1996). In some experiments, we observed that picrotoxin's effect was incomplete, which is consistent with the properties of glutamate-gated chloride conductances in other species (Barbara et al., 2005; Raymond et al., 2000). The concentration of picrotoxin we needed to achieve this level of blockade was higher than that needed to block GABA-gated chloride conductances in the same neurons (Wilson and Laurent, 2005a), but we were not able to find a picrotoxin concentration that would completely block GABA-gated conductances without affecting glutamate-gated conductances.

To test whether the glutamate-gated conductance in antennal lobe neurons requires the *GluClα* gene, we used Gal4/UAS to express an RNAi hairpin targeting *GluClα* specifically in antennal lobe PNs, and we co-expressed GFP in these neurons to mark them for recording. In control experiments, the RNAi hairpin transgene was omitted. We found that *GluClα* knockdown

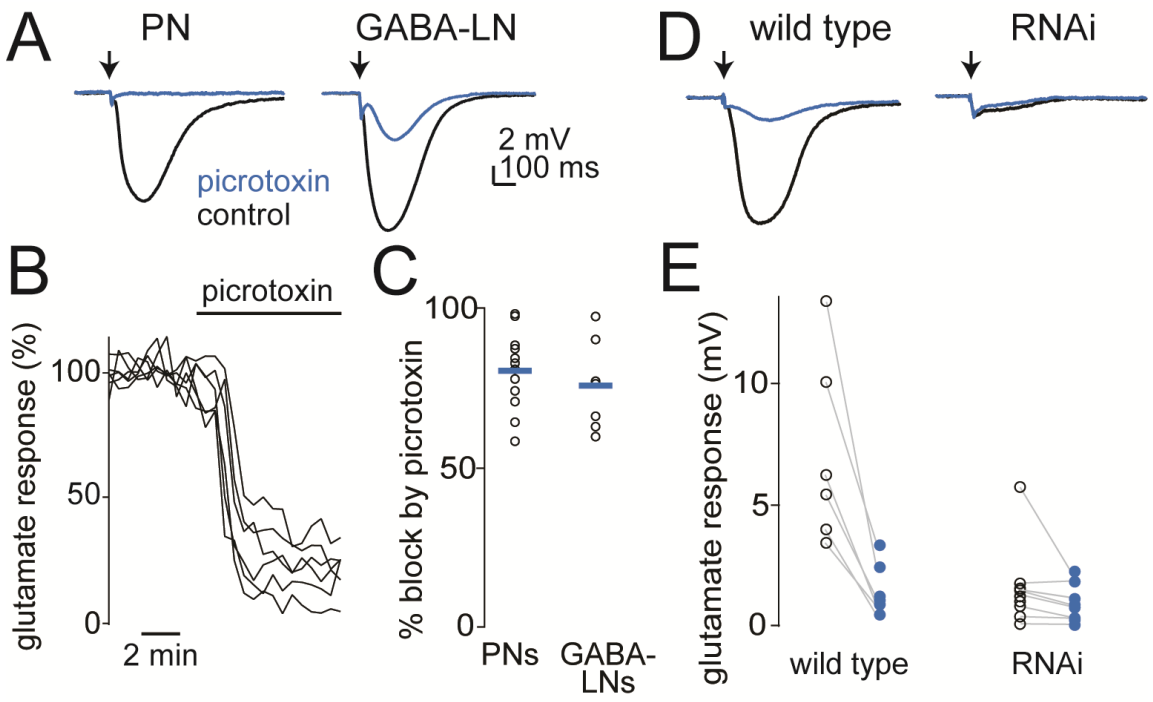

Figure 3.3: GluClα mediates a glutamate-gated chloride conductance in PNs and GABAergic LNs.

(A) Whole-cell current-clamp recording from the soma of an antennal lobe PN (left) and a GABA-LN (right). A pulse of glutamate in the antennal lobe neuropil (arrow, 10 – 20 ms) hyperpolarizes both cells. Picrotoxin (100 µM) either abolishes or attenuates the response, depending on the recording.
(B) Time course of the effect of picrotoxin on glutamate responses in in PNs, normalized to baseline in each cell. Each line represents a different PN recording.
(C) Effect of picrotoxin in reducing responses to glutamate. Each symbol is a different recording, with means in blue. Overall, the effects of picrotoxin were similar in PNs (n = 12) and GABAergic LNs (n = 7).
(D) Responses to glutamate before and after applying 100µM picrotoxin in a wild type PN (left) and a PN expressing *GluClα* RNAi (right). Arrow indicates iontophoretic pulses. The residual deflection is a stimulus artifact.
(E) Hyperpolarizing responses to iontophoresis in both genotypes, before picrotoxin (black) and after picrotoxin (blue). The response to glutamate is significantly smaller in RNAi flies versus wild type ($P < 0.05$, t-test, n = 6 wild type and 9 RNAi). The percent inhibition by picrotoxin is also significantly smaller ($P < 0.0001$, t-test).

virtually abolished the response to iontophoresed glutamate (Fig. 3.3D,E). As a control, we verified that *GluClα* knockdown did not reduce responses to GABA-gated currents in PNs (Fig. 3.4).

We never observed a depolarizing response to glutamate in these recordings. This was true even when picrotoxin was present, and when *GluClα* expression was knocked down. Moreover, ionotropic glutamate receptor antagonists CNQX (10 μM) and MK801 (100 μM) had no effect on the response to iontophoresed glutamate. The metabotropic glutamate receptor antagonist LY341495 (1 μM) also had no effect.

Glutamatergic LNs inhibit PNs

We next investigated the effects of endogenous glutamate on antennal lobe PNs. To selectively stimulate glutamatergic LNs, we misexpressed an ATP-gated cation channel (P2X2) under the control of *OK371-Gal4*. Because there are no native *Drosophila* channels gated by ATP (Littleton and Ganetzky, 2000), applying ATP should selectively depolarize the neurons that express Gal4 (Lima and Miesenbock, 2005). In these experiments, we also co-expressed GFP with P2X2 in order to mark these neurons. As expected, Glu-LNs were depolarized by brief ATP pressure ejection (Fig. 3.5A), but only when the Gal4 transgene was present (see Experimental Procedures). Based on the number of neurons in the vicinity of the ejection pipette that express Gal4, we estimate that several dozen Glu-LNs are being depolarized simultaneously.

We found that PNs were inhibited by selectively stimulating Glu-LNs. Specifically, in whole-cell recordings from PNs, the membrane potential was hyperpolarized and spontaneous spiking paused (Fig. 3.5B-D). These effects were blocked by picrotoxin (Fig. 3.5B,E). As a control, we verified that these effects were absent when the Gal4 transgene was omitted (see Experimental Procedures).

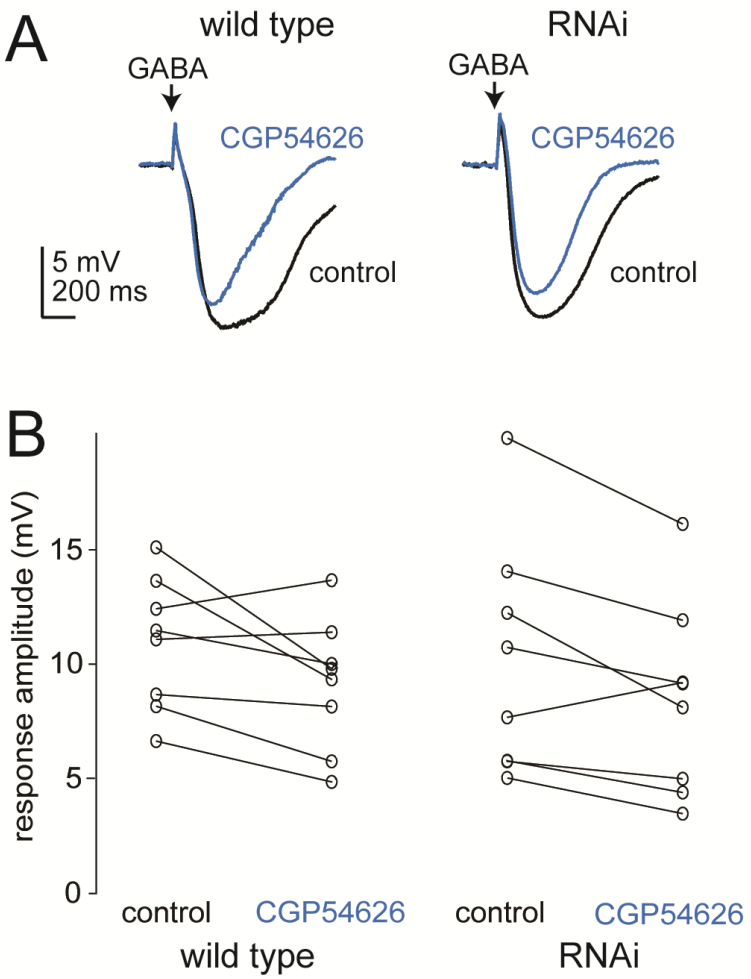

Figure 3.4: GluClα knockdown does not affect PN responses to GABA.

(A) Whole-cell recordings from an antennal lobe PN in a wild type fly (left) and a fly where the *GluClα* RNAi construct is expressed specifically in PNs (right). A pulse of GABA in the antennal lobe neuropil (arrow) hyperpolarizes the PN in both cases. CGP54626 (50 µM) blocks the $GABA_B$ component of these responses, and what remains is the $GABA_A$ component (Wilson and Laurent, 2005a). Note that the responses to GABA are similar in the two cells, as is the fractional block by CGP54626.
(B) Group data showing responses to GABA iontophoresis in all experiments, before and after adding CGP54626. The percent inhibition by CGP54626 is not significantly different in the control and RNAi genotype (P = 0.97, t-test). This demonstrates that the RNAi construct is specific for *GluClα* and does not affect GABA receptors.

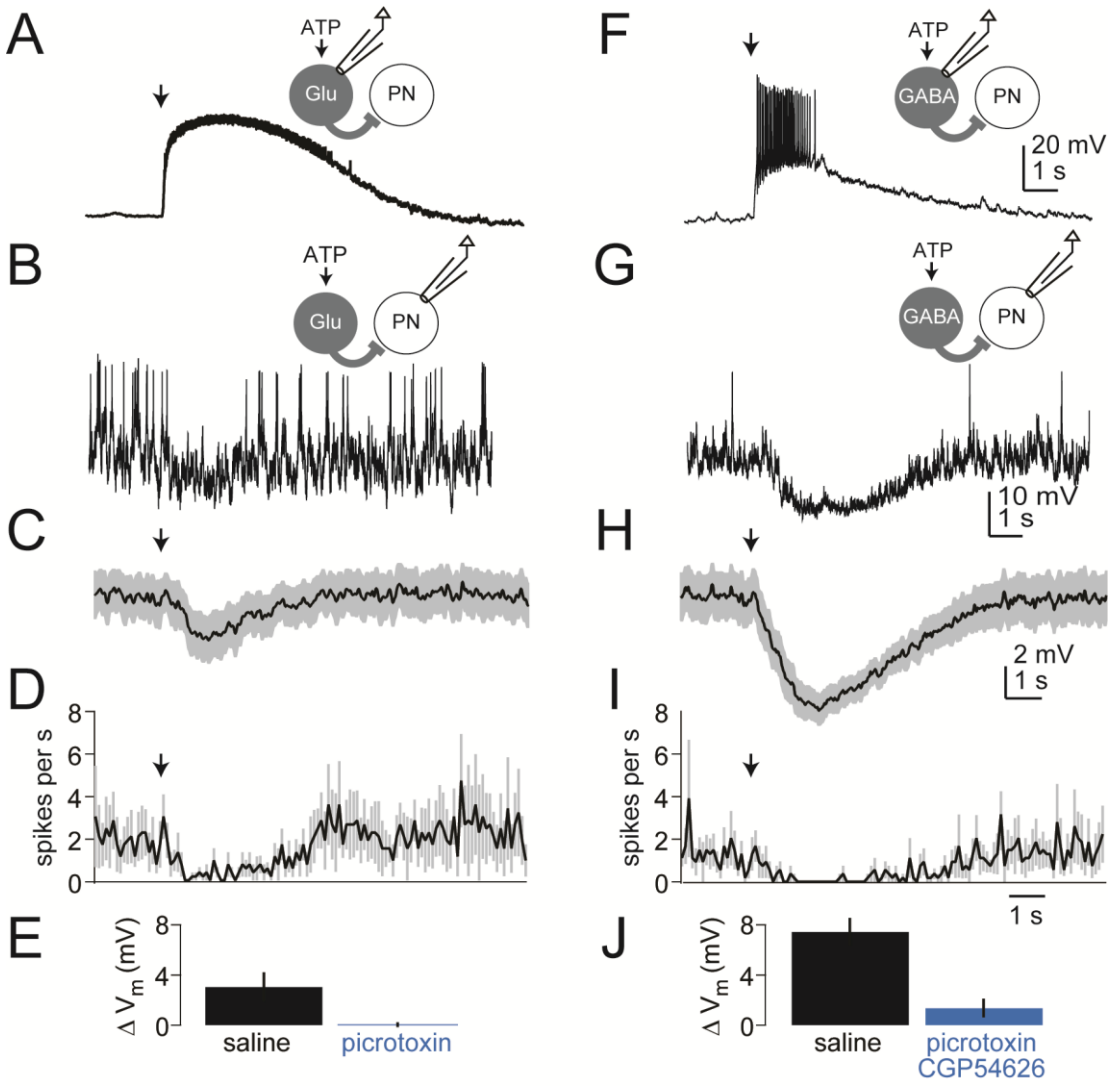

Figure 3.5: PNs are inhibited by stimulation of either Glu-LNs or GABA-LNs.

(A) A recording from a P2X2-expressing Glu-LN, showing that ATP ejection (arrow) depolarized the cell and elicited a train of short spikes.
(B) A recording from a PN showing that, when Glu-LNs were stimulated with ATP (arrow), spontaneous spiking paused and the membrane was slightly hyperpolarized (top).
(C) Mean membrane potential of PNs in response to Glu-LN stimulation, averaged across experiments, ± SEM (n = 13).
(D) Mean firing rate of PNs in response to Glu-LN stimulation, averaged across experiments, ± SEM (n = 9; some cells were excluded because they did not spike during the analysis window).
(E) Mean membrane potential change of PNs in response to Glu-LN stimulation, averaged across experiments, ± SEM. Picrotoxin significantly reduced the response to Glu-LN stimulation (P < 0.05, paired t-test, n = 4).
(F-J) Same as above, but this time stimulating GABA-LNs rather than Glu-LNs (n = 13 for H and J, and n = 9 for I). Picrotoxin (5 µM) and CGP54626 (50 µM) significantly reduced the membrane potential change in response to GABA-LN stimulation (P = 0.01, paired t-test, n = 8).

For comparison, we used the same technique to selectively stimulate GABA-LNs. We expressed P2X2 in a large population of GABA-LNs under the control of *NP3056-Gal4*, and we verified that ATP depolarizes these neurons (Fig. 3.5F). We found that GABA-LNs and Glu-LNs had similar effects on PNs; specifically, the membrane potential was hyperpolarized and spiking paused (Fig. 3.5-I). As expected, inhibition by GABA-LNs was blocked by the $GABA_A$ antagonist picrotoxin and the $GABA_B$ antagonist CGP54626 (Fig. 3.5J).

Together, these results indicate that Glu-LNs can inhibit PNs, similar to the effects of GABA-LNs on PNs. Although glutamate release is not concentrated within glomeruli, co-activation of multiple Glu-LNs is sufficient to produce robust effects on PNs, possibly due to pooling of glutamate from multiple LNs.

Glutamatergic LNs inhibit GABAergic LNs

We next asked whether Glu-LNs can inhibit GABA-LNs. This experiment was motivated by our observation that iontophoresed glutamate hyperpolarizes GABA-LNs (Fig. 3.3). As before, we drove P2X2 expression specifically in Glu-LNs, and we stimulated Glu-LNs with ATP. Recordings from GABA-LNs showed that they were hyperpolarized and spontaneous firing was suppressed (Fig. 3.6A-C). These effects were abolished by picrotoxin (Fig. 3.6D).

We then repeated this experiment, but this time stimulating GABA-LNs rather than Glu-LNs. As in all these experiments, we co-expressed GFP with P2X2, and so could identify non-P2X2-expressing cells by their lack of GFP expression. We could therefore stimulate some GABA-LNs while recording from other GABA-LNs that were not directly stimulated. These recordings showed robust inhibition (Fig. 3.6E-G) which was blocked by picrotoxin and CGP54626 (Fig. 3.6H).

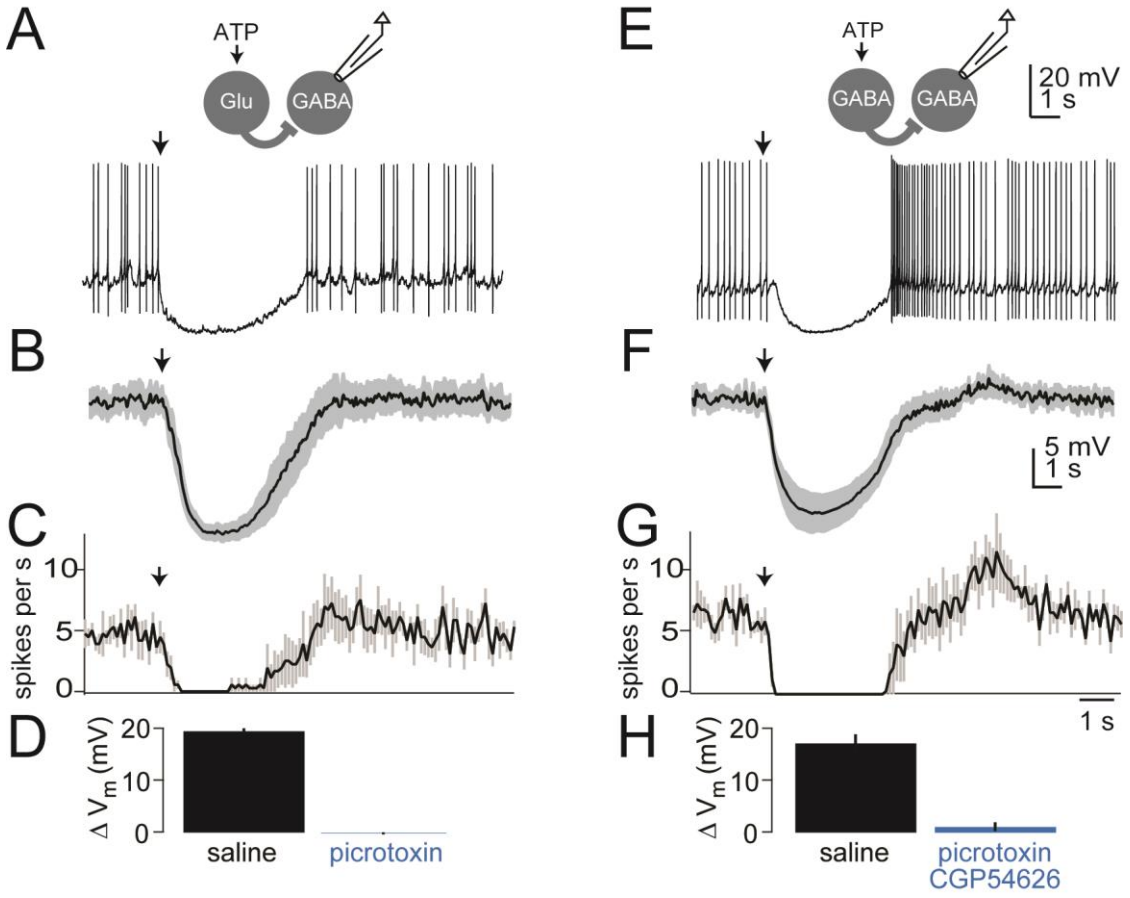

Figure 3.6: GABA-LNs are inhibited by stimulation of either Glu-LNs or GABA-LNs.

(A) A GABA-LN recording. When Glu-LNs were stimulated with ATP (arrow), spontaneous spiking paused and the membrane potential hyperpolarized.
(B) Mean membrane potential of GABA-LNs in response to Glu-LN stimulation, averaged across experiments, +/- SEM (n = 6).
(C) Mean firing rate of GABA-LNs in response to Glu-LN stimulation, averaged across experiments, ± SEM (n = 6).
(D) Mean membrane potential change of GABA-LNs in response to Glu-LN stimulation, averaged across experiments, ± SEM. Picrotoxin significantly reduced the response to Glu-LN stimulation ($P < 0.001$, paired t-test, n = 4).
(E-H) Same as above, but this time stimulating GABA-LNs rather than Glu-LNs. Picrotoxin (100 µM) and CGP54626 (50 µM) significantly reduced the response to GABA-LN stimulation (P =0.001, paired t-test, n = 5). Although GABA-LNs lack $GABA_B$ conductances (Wilson and Laurent, 2005a), CGP54626 was needed to produce complete block; GABA-LN stimulation may inhibit tonically active ORNs and PNs via both $GABA_A$ and $GABA_B$ receptors, thereby reducing tonic excitation to GABA-LNs.

Thus, GABA-LNs receive inhibition from both Glu-LNs and other GABA-LNs. This is further evidence that glutamate and GABA function in parallel as inhibitory neurotransmitters.

Paired recordings reveal connections made by individual glutamatergic and GABAergic neurons

We next used paired whole-cell recordings to investigate the connectivity of individual LNs. In every paired recording, we injected depolarizing current into one cell while monitoring the response of the non-stimulated cell. LNs do not have axons, and PNs do not make axonal synapses in the antennal lobe, and so connections between these neurons must represent dendro-dendritic interactions.

In these recordings, the highest rate of connectivity was observed between GABA-LNs and PNs. In most cases, depolarizing the GABA-LN hyperpolarized the PN (Fig. 3.7A), and these responses were abolished by CGP54626. This confirms previous findings that GABA-LNs inhibit PNs in paired recordings (Yaksi and Wilson, 2010). In most cases, these connections were reciprocal: depolarizing the PN depolarized the GABA-LN (Fig. 3.7B). These connections were blocked by the nicotinic antagonist mecamylamine, consistent with the fact that PNs are cholinergic (Yaksi and Wilson, 2010).

Next, we performed paired recordings from Glu-LNs and PNs (Fig. 3.7C,D). We did not detect any connections from Glu-LNs onto PNs in 65 pairs. This is significantly different from the connection rate in paired recordings with GABA-LNs and PNs ($P < 0.001$, two-sample binomial test). Our failure to detect these connections is difficult to explain by postulating a low rate of connectivity: even if each PN received input from only 5 out of the ~70 Glu-LNs, obtaining zero hits in 65 attempts is improbable ($P < 0.01$, binomial test). This suggests that multiple Glu-LNs must be co-activated in order to inhibit a PN, which could indicate that glutamate must diffuse some distance before activating receptors on PNs.

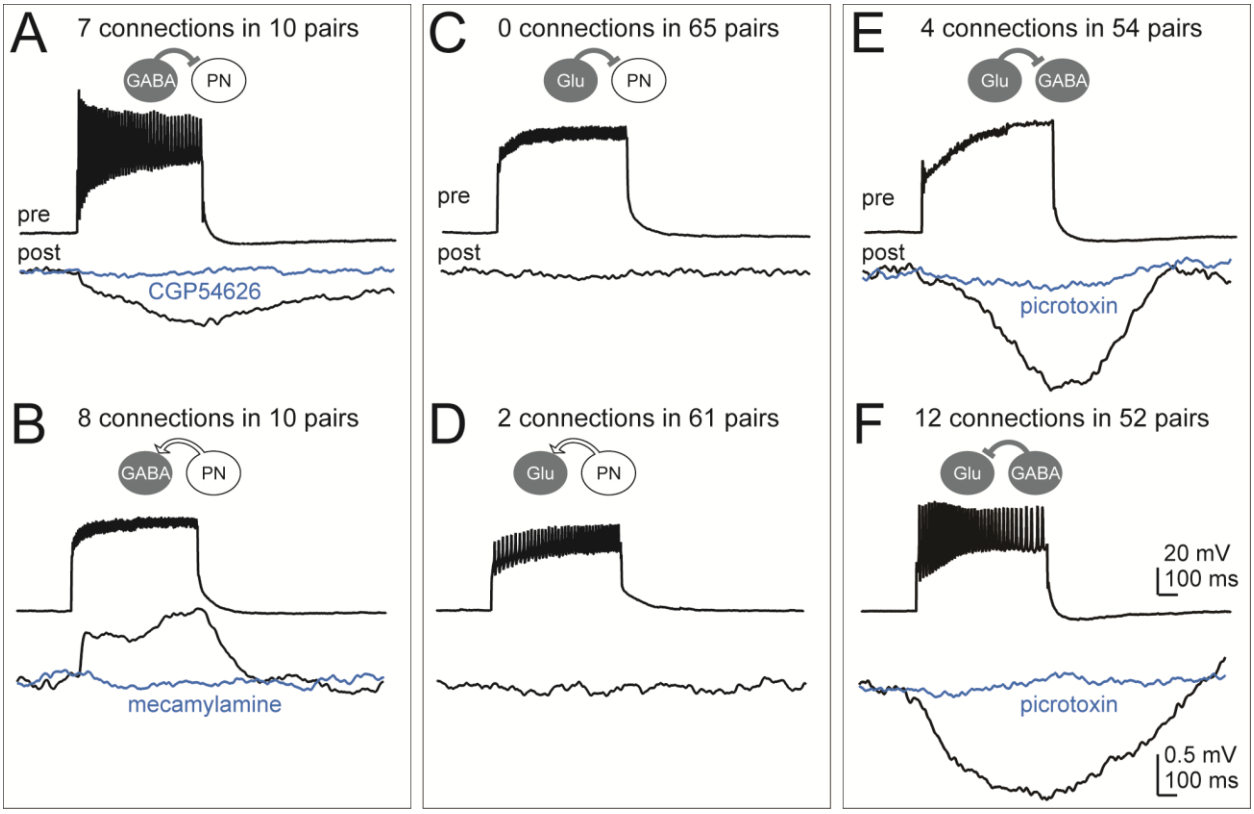

Figure 3.7: Paired recordings reveal the connectivity of individual LNs.

(A) An example of an inhibitory connection from a GABA-LN onto a PN. Depolarizing current was injected into the GABA-LN through the patch electrode (pre, single trial). CGP54626 (50 µM) blocked the response in the PN (post, mean of 50-60 trials).
(B) An example of an excitatory connection from a PN onto a GABA-LN. Mecamylamine (50 µM) blocked the response. Scale bars apply to all panels in this figure.
(C) In a typical paired recording, there was no effect of stimulating a Glu-LN on a PN.
(D) Similarly, in the same pair, there was no effect of stimulating the PN on the Glu-LN. The total number of pairs tested is not identical to C because a few recordings were lost before both directions of connectivity could be tested.
(E) An example of an inhibitory connection from a Glu-LN onto a GABA-LN. Note that the presynaptic spikes are very small, which is typical of many Glu-LNs. Picrotoxin (100 µM) blocked the response.
(F) An example of an inhibitory connection from a GABA-LN onto a Glu-LN. Picrotoxin (5 µM) blocked the response.

Our results were similar when we probed for connections in the other direction, from PNs onto Glu-LNs. Consistent with the idea that PNs and Glu-LNs are generally not in direct contact, we observed no connections except in two isolated cases. In one case, depolarizing the PN produced a depolarization in the Glu-LN, and this was blocked by the nicotinic antagonist mecamylamine. In the other case, the Glu-LN was hyperpolarized, and this was blocked by the muscarinic antagonist atropine.

Finally, we performed paired recordings from Glu-LNs and GABA-LNs. In several of these pairs, depolarizing the Glu-LN elicited a hyperpolarization in the GABA-LN (Fig. 3.7E) which was blocked by picrotoxin. Conversely, depolarizing the GABA-LN elicited a hyperpolarization in the Glu-LN in several of the pairs we recorded from (Fig. 3.7F), and this was also blocked by picrotoxin. These data show that individual Glu-LNs and GABAergic LNs can mutually inhibit each other.

Glutamate inhibits ORN-to-PN synapses

GABA can inhibit neurotransmitter release from the axons of olfactory receptor neurons (ORNs) in the antennal lobe (Olsen and Wilson, 2008b; Root et al., 2008). We therefore investigated whether glutamate can play the same role. We made voltage-clamp recordings from PNs while electrically stimulating the ipsilateral antennal nerve to evoke excitatory postsynaptic currents (EPSCs). We then iontophoresed glutamate into the antennal lobe neuropil, and found that glutamate inhibited evoked EPSCs (Fig. 3.8A,B). The inhibition of EPSCs was reduced by picrotoxin (Fig. 3.8B), implying that glutamate-gated chloride channels contribute to the inhibition.

To ask whether there is a presynaptic contribution to this effect, we used paired-pulse stimulation of the antennal nerve. We delivered a pair of pulses in quick succession, and

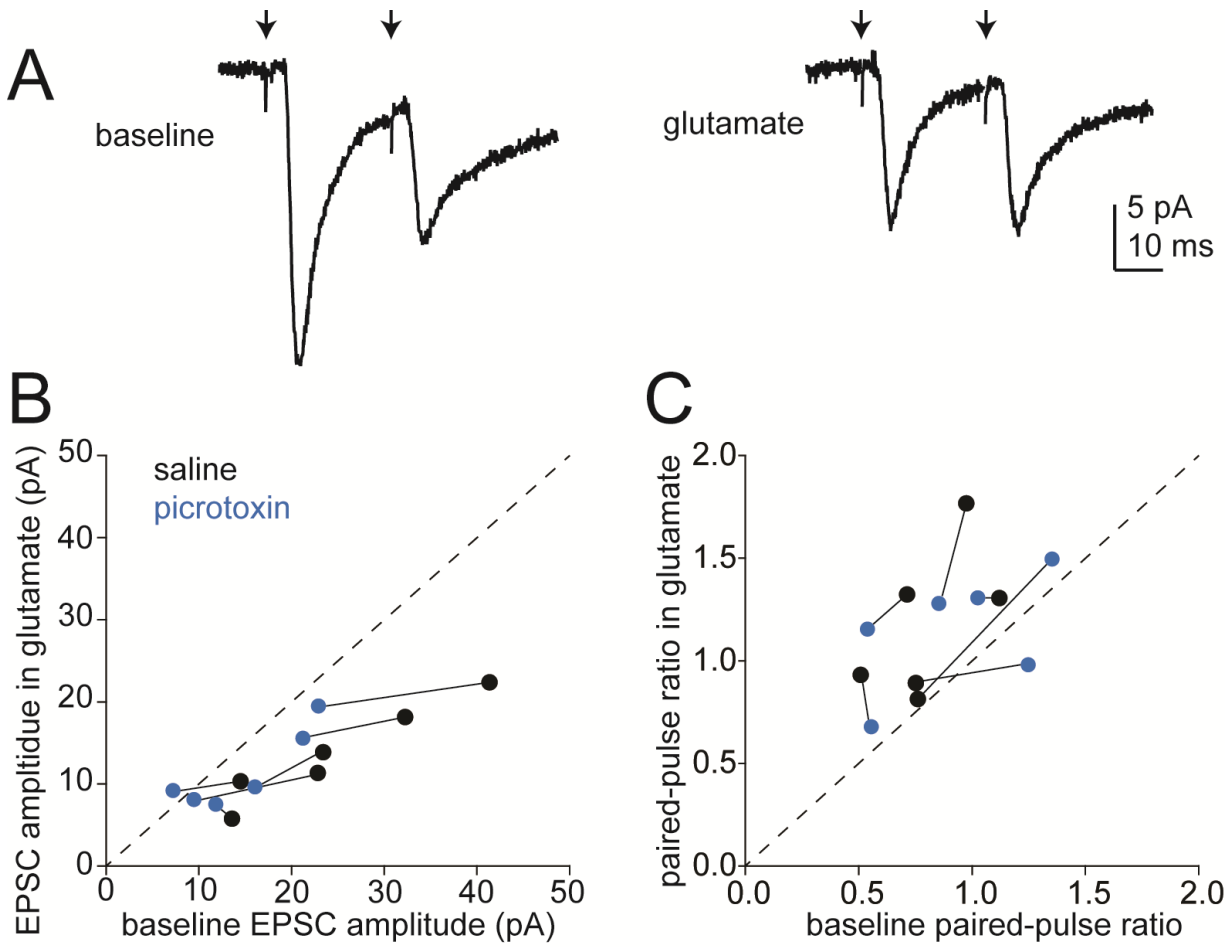

Figure 3.8: Glutamate inhibits ORN-to-PN synapses.

(A) A voltage-clamp recording from a PN shows EPSCs evoked by stimulation of ORN axons in the antennal nerve with a pair of electrical pulses (arrows). Glutamate iontophoresis inhibits the amplitude of the evoked EPSCs. Glutamate also increases the paired-pulse ratio (EPSC2/EPSC1). Traces are averages of 14 trials.
(B) Summary of the effects of glutamate on EPSC1, where each symbol is a different experiment. Glutamate significantly inhibits EPSC1 amplitude ($P < 0.005$, 2-way repeated measures ANOVA, n = 6). The magnitude of inhibition by glutamate is significantly reduced by 100 μM picrotoxin (blue symbols, $P < 0.01$, 2-way repeated measures ANOVA). Lines connect symbols corresponding to the same experiment.
(C) Summary of the effects of glutamate on paired-pulse ratios. Glutamate significantly increases PPR ($P < 0.05$, n = 6), Picrotoxin does not significantly change the effect of glutamate on PPR ($P = 0.19$, 2-way repeated measures ANOVA).

computed the paired pulse ratio (PPR, defined as $EPSC_2/EPSC_1$). Manipulations that decrease presynaptic vesicular release probability generally increase PPR (Zucker and Regehr, 2002). We observed that glutamate increased PPR (Fig. 3.8A,C), indicating that the inhibition of EPSCs is at least partly presynaptic. However, picrotoxin did not significantly alter the effect of glutamate on the PPR (Fig. 3.8C). This may reflect incomplete blockade of glutamate-gated chloride channels by picrotoxin (Fig. 3.3D), or an additional contribution to presynaptic inhibition from other glutamate receptors (e.g., a metabotropic glutamate receptor).

These data demonstrate that glutamate can inhibit neurotransmitter release from ORN axons, similar to the action of GABA. This effect appears to be at least partly mediated by glutamate-gated chloride conductances, although metabotropic glutamate receptors may also contribute to presynaptic inhibition.

Eliminating glutamatergic inhibition in PNs disinhibits odor responses

Finally, we asked whether glutamatergic inhibition makes a functional contribution to PN odor responses. To investigate this, we knocked down *GluClα* expression in PNs. Gal4/UAS was used to express an RNAi hairpin against *GluClα* specifically in antennal lobe PNs, and GFP was co-expressed in these neurons to mark them for recording. In control experiments, the RNAi hairpin transgene was omitted. We filled each recorded PN with biocytin and used *post hoc* confocal microscopy to identify the glomerulus it innervated.

We recorded from 29 PNs in total in these experiments. PNs from four different glomeruli appeared in both the control data set and the RNAi data set. Because PNs in different glomeruli have diverse odor responses, meaningful between-experiment comparisons can only be made by comparing results for identified PNs. Therefore, we analyzed only the four PN types corresponding to the four glomeruli that appeared in both data sets: DL1, VM2, VM5 and VA1v.

Figure 3.9: Odor responses are disinhibited by knockdown of GluClα in PNs.

(A) Odor responses of PNs in four different glomeruli. The membrane potential is low-pass filtered to remove spikes. Each trace represents a different recording, with 10 PNs total. In half of these experiments (blue traces), we used transgenic RNAi to knock down *GluClα* expression specifically in PNs. Black traces are wild type. Some panels show two traces in the same color because we recorded from two PNs in that glomerulus for that genotype. Responses are averaged across 5-6 trials. Odor stimuli are pentyl acetate 10^{-2} (VM2, VM5, VA1v) and methyl salicylate 10^{-2} (DL1). For simplicity, we analyzed only the stimulus that produced the largest response in each PN type, although all odor responses were affected similarly.
(B) Peristimulus time histograms showing spiking responses of the same PNs.
(C) Mean odor-evoked changes in membrane potential (averaged over the 2-s stimulus period) in all cells. Each symbol represents a different recording (n = 5 control, n = 5 RNAi). Responses in wild type (black) and RNAi flies (blue) are significantly different ($P < 0.001$, 2-way ANOVA). The values for the two wild type VM5 recordings are so similar that their symbols lie on top of one another.
(D) Mean odor-evoked firing rates for the same cells. Responses in wild type and RNAi flies are significantly different ($P < 0.005$, 2-way ANOVA).
(E) Schematic showing interactions between PNs, and LNs in the two genotypes. Some connections are omitted for clarity.

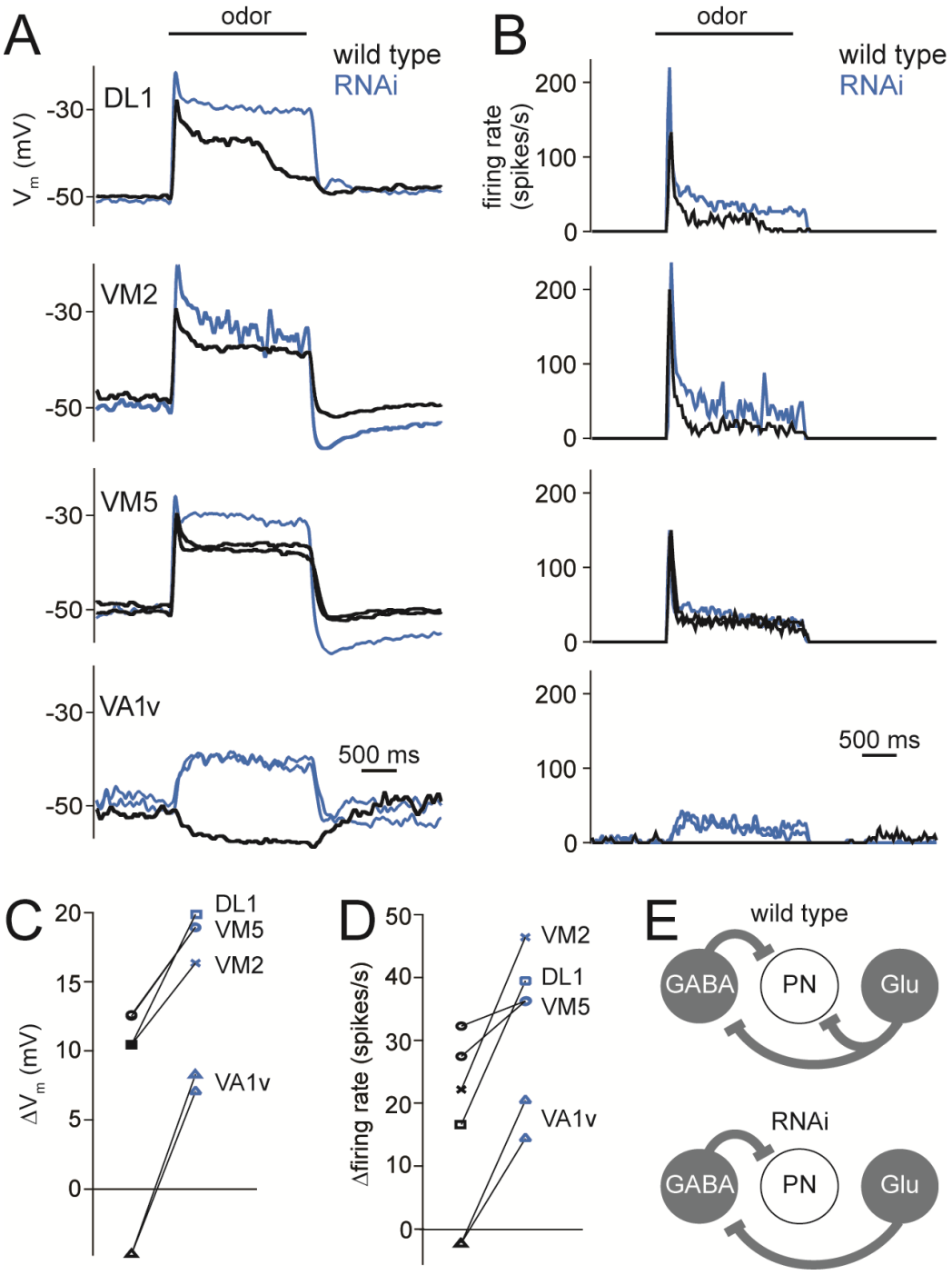

Figure 3.9: Odor responses are disinhibited by knockdown of *GluClα* in PNs (continued).

Knocking down *GluClα* in these PNs systematically disinhibited all odor responses (Fig. 3.9A,B). Odor-evoked excitatory responses were increased, and in one PN type (VA1v), odor-evoked inhibition was converted to odor-evoked excitation (Fig. 3.9C,D). These results demonstrate that glutamatergic inhibition makes a measurable contribution to the output of the antennal lobe, and that its direct effect on PNs is inhibitory.

Discussion

Glutamate as an inhibitory neurotransmitter acting via GluClα

Although glutamatergic neurons are abundant in the *Drosophila* brain (Daniels et al., 2008), the role of glutamate as a neurotransmitter in the *Drosophila* CNS has received little study. In the antennal lobe, where about one-third of LNs are glutamatergic (Chou et al., 2010a; Das et al., 2011a), the physiological effects of glutamate have never been characterized. In this study, we show that glutamate is an inhibitory transmitter in the antennal lobe, and that glutamate shapes the responses of PNs to olfactory stimuli.

In the past, glutamate has been proposed to mediate lateral excitation between olfactory glomeruli (Das et al., 2011a). Our results demonstrate that the main effect of glutamate is inhibition, not excitation. We cannot rule out the possibility that glutamate has small excitatory effects in the antennal lobe which are masked by its inhibitory effects, but we could not find evidence of excitation even when *GluClα* was knocked down genetically or inhibited pharmacologically. We note that there is in fact lateral excitation in the antennal lobe, which exists in parallel with lateral inhibition (Olsen et al., 2007; Shang et al., 2007). However, lateral excitation is mediated not by glutamate, but by electrical coupling between LNs and PNs (Huang et al., 2010; Yaksi and Wilson, 2010).

We found that all the effects of glutamate on PNs were eliminated by knocking down *GluClα*. The dominant role for *GluClα* is notable, given how many other glutamate receptors are encoded in the genome. Our results are particularly surprising in light of two recent studies that have reported behavioral effects of knocking down an NMDA receptor subunit (*NR1*) in antennal lobe PNs (Das et al., 2011b; Sudhakaran et al., 2012). Further experiments will be needed to clarify how *NR1* might affect PN function.

There is a precedent for the idea that glutamate can be an inhibitory neurotransmitter in the *Drosophila* brain. Specifically, several studies have reported that bath-applied glutamate inhibits the large ventrolateral neurons of the *Drosophila* circadian clock circuit (Collins et al., 2012; Hamasaka et al., 2007; McCarthy et al., 2011). Collectively, these studies suggest roles for both ionotropic and metabotropic glutamate receptors in glutamatergic inhibition. Regardless of which glutamate receptors are involved, these studies are consistent with the conclusion that glutamate is an important mediator of synaptic inhibition.

The idea that glutamate can be inhibitory has important implications for neural coding. One particularly interesting case is the motion vision circuit of the *Drosophila* optic lobe. Two neuron types, L1 and L2, both receive strong synaptic inputs from photoreceptors, and they respond equally to contrast increments ("on") and decrements ("off") (Clark et al., 2011). However, based on conditional silencing experiments, L1 is thought to provide input to an "on" pathway, and L2 to an "off" pathway (Joesch et al., 2010). Therefore, opponency must arise downstream from L1 and L2 (Clark et al., 2011; Joesch et al., 2010). According to recent evidence, L1 is glutamatergic, while L2 is cholinergic (Takemura et al., 2011). In light of our data, that result suggests that L1 may actually be inhibitory, which would be sufficient to create opponency in the “on” and “off” pathways.

Glutamate can act as an inhibitory neurotransmitter in the *C. elegans* olfactory circuit, and this too has implications for neural coding of odors in this organism. In the worm, a specific type of glutamatergic olfactory neuron inhibits one postsynaptic neuron via GluCl, while also exciting another postsynaptic neuron via an AMPA-like receptor. This creates a pair of opponent neural channels which respond in an anti-correlated fashion to odor presentation or odor removal (Chalasani et al., 2007), analogous to opponent channels in the visual system.

Comparisons between glutamatergic and GABAergic inhibition

We have shown that the cellular actions of Glu-LNs are broadly similar to the actions of GABA-LNs. Specifically, both types of LNs inhibit PNs, as well as other LNs. In addition, we found that both GABA and glutamate inhibit neurotransmitter release from ORNs (Fig. 3.8). Thus, both neurotransmitters inhibit all the major cell types in the antennal lobe circuit.

However, Glu-LNs and GABA-LNs are not functionally identical. In particular, we found that the vesicular glutamate transporter is mainly confined to the spaces between glomeruli, whereas the vesicular GABA transporter is abundant within glomeruli. This implies that glutamate and GABA are released in largely distinct spatial locations. Consistent with this, we observed no individual synaptic connections from Glu-LNs onto PNs, whereas we observed a substantial rate of connections from GABA-LNs onto PNs. Nevertheless, our data clearly indicate that endogenous glutamate can inhibit PNs directly via GluCl: we found that PNs are hyperpolarized by co-activation of multiple Glu-LNs, and PNs are disinhibited by knockdown of GluCl specifically in PNs.

These results can be reconciled by a model where the sites of glutamate release are distant from PN glutamate receptors. As a result, glutamate would need to diffuse some distance to inhibit PNs. Co-activation of multiple Glu-LNs would increase extracellular glutamate

concentrations, overwheming uptake mechanisms and allowing glutamate to diffuse further. In this scenario, glutamatergic inhibition should be most important when LN activity is intense and synchronous. By comparison, GABAergic inhibition of PNs does not require LN co-activation, implying a comparatively short distance between pre- and postsynaptic sites. There is a precedent in the literature for the idea that different forms of inhibition can be differentially sensitive to LN co-activation, due to the spatial relationship between pre- and postsynaptic sites. In the hippocampus, $GABA_A$ receptors are closer than $GABA_B$ receptors to sites of GABA release, and so activation of individual interneurons produces $GABA_A$ but not $GABA_B$ currents, whereas co-activation of many interneurons produces both $GABA_A$ and $GABA_B$ currents (Scanziani, 2000).

The pharmacology of glutamate-gated conductances in antennal lobe neurons is similar to the pharmacology of $GABA_A$ conductances in these neurons. This should prompt a reevaluation of studies that used picrotoxin to block inhibition in the antennal lobe (Olsen et al., 2010; Olsen and Wilson, 2008b; Root et al., 2008; Silbering and Galizia, 2007; Wilson and Laurent, 2005a; Wilson et al., 2004). Given our results, it seems likely that these studies were reducing both glutamatergic and GABAergic inhibition.

Interactions between glutamatergic and GABAergic inhibition

It is perhaps surprising that knocking down *GluClα* in PNs had such a substantial effect on PN odor responses, given that picrotoxin alone has comparatively modest effects (Olsen and Wilson, 2008b; Root et al., 2008; Silbering and Galizia, 2007; Wilson and Laurent, 2005a; Wilson et al., 2004). The solution to this puzzle may lie in our finding that glutamate regulates not only PNs but also GABA-LNs. Importantly, GABA-LNs are spontaneously active and provide tonic inhibition to PNs (Chou et al., 2010a; Wilson and Laurent, 2005a). Hence, in the

intact circuit, glutamatergic inhibition of GABA-LNs should tend to disinhibit PNs (Fig. 3.9E). Picrotoxin prevents Glu-LNs from inhibiting GABA-LNs, and so should tend to potentiate GABAergic inhibition. The effects of GABA are mediated in part by $GABA_B$ receptors, which are not sensitive to picrotoxin. Thus, picrotoxin likely has bidirectional effects on the total level of inhibition in the circuit. By contrast, knockdown of *GluClα* specifically in PNs should not directly affect GABA-LNs, and so should not produce these complex effects (Fig. 3.9E). These results illustrate how a cell-specific genetic blockade of a neurotransmitter system can have more dramatic effects than a global pharmacological blockade of the same system.

Our study reveals that an LN can have push-pull effects on a single population of target cells. For example, Glu-LNs directly inhibit PNs, but they should also tend to disinhibit PNs, via the inhibition of GABA-LNs. This may allow for more robust gain control, and rapid transitions between network states. This arrangement is similar to the wiring of many cortical circuits, where co-recruitment of excitation and inhibition is a common motif (Isaacson and Scanziani, 2011).

Why might the existence of two parallel inhibitory transmitters be useful? Our data argue that GABA and glutamate may act on different spatial and temporal scales. Because these two inhibitory systems comprise different cells, receptors, and transporters, they can be modulated independently. And, because their properties are encoded by different genes, they can also evolve independently. This should confer increased flexibility in adapting synaptic inhibition to a changing environment.

Experimental Procedures

Fly stocks

Flies were raised on standard cornmeal agar medium supplemented with potato food on a 12 h light/dark cycle at 25°C. All experiments were performed on adult female flies 1-4 days post eclosion. The only exceptions were the experiments examining the effect of *GluClα* knockdown, where both control and RNAi flies were male. The genotypes used were as follows: Figures 3.1B-C - *OK371-Gal4/UAS-CD8:GFP*; Figure 3.1D-E - *pebbled-Gal4/+;UAS-nsyb:GFP/+*; Figure 3.2 - *OK371-Gal4/UAS-CD8:GFP*; Figure 3.3A-D - *GH146-Gal4,UAS-CD8:GFP*; Figures 3.3D-E and 3.4- *UAS-dicer2/Y;GH146-Gal4,UAS-CD8:GFP/+* (wild type) and *UAS-dicer2/Y;GH146-Gal4,UAS-CD8:GFP/ UAS-GluClα RNAi* (RNAi); Figures 3.5 and 3.6 - *OK371-Gal4,UAS-CD8:GFP/UAS-CD8:GFP;UAS-P2X2/+* (Glu-LN stimulation) and *UAS-CD8:GFP; UAS-P2X2/NP3056-Gal4* (GABA-LN stimulation); Figure 3.7 - *OK371-Gal4,UAS-CD8:GFP*; Figure 3.8 - *GH146-Gal4,UAS-CD8:GFP*; Figure 3.9 - *UAS-dicer2/Y;GH146-Gal4,UAS-CD8:GFP/+* (wild type) and *UAS-dicer2/Y;GH146-Gal4,UAS-CD8:GFP/UAS-GluClα RNAi* (RNAi). Fly stocks were previously published as follows: *OK371-Gal4* (II) (Mahr and Aberle, 2006), *UAS-CD8:GFP* (II and III) (Lee and Luo, 1999), *pebbled-Gal4* (X) (Sweeney et al., 2007), *UAS-nsyb:GFP* (Zhang et al., 2002), *GH146-Gal4* (II) (Stocker et al., 1997), *UAS-P2X2* (III) (Lima and Miesenbock, 2005), *NP3056-Gal4* (III) (Chou et al., 2010a), *UAS-GluClα RNAi* (II) (Collins et al., 2012; Dietzl et al., 2007), *UAS-dicer2* (X) (Dietzl et al., 2007). Stocks of *OK371-Gal4*, *UAS-CD8:GFP* (II and III), *UAS-nsyb:GFP*, and *UAS-dicer2* were obtained from the Bloomington Drosophila Stock Center. The *UAS-GluClα RNAi* insertion that we used in this study has been previously shown to substantially reduce *GluClα* RNAi levels in adult brain tissue (Collins et al., 2012), and we verified that it does not affect responses to iontophoresed GABA in these neurons (Fig. 3.4). However, it is difficult to completely exclude the possibility of off-target effects, given the lack of available alternative

reagents for cross-validation. The *UAS-GluClα RNAi* insertion was obtained from the Vienna Drosophila RNAi Center (transformant ID 105754, sequence details available at http://stockcenter.vdrc.at).

Electrophysiological recordings

In vivo whole-cell patch clamp recordings were performed essentially as previously described (Wilson and Laurent, 2005a; Wilson et al., 2004). In order to perform recordings from Glu-LNs, the head was rotated 180º around the thin neck connective, so that the ventral side of the brain was facing upwards and therefore accessible to visualization via the water-immersion objective above the preparation. The fly remained alive even when the head was rotated in this manner. The brain was perfused in external saline containing (in mM): 103 NaCl, 3 KCl, 5 N-tris(hydroxymethyl) methyl-2-aminoethane-sulfonic acid, 8 trehalose, 10 glucose, 26 $NaHCO_3$, 1 NaH_2PO_4, 1.5 $CaCl_2$, and 4 $MgCl_2$ (osmolarity adjusted to 270-275 mOsm). The saline was bubbled with 95% O_2/ 5% CO_2 to a pH of 7.3. The internal solution for patch-clamp pipettes were contained the following (in mM): 140 potassium aspartate, 10 HEPES, 1EGTA, 4 MgATP, 0.5 Na_3GTP, 1 KCl, and 13 biocytin hydrazide. The pH of the internal solution was adjusted to 7.2 and the osmolarity was adjusted to ~265 mOsm. In cases where antennal lobe PNs and GABA-LNs were not labeled with GFP, they were identified based on the location and size of their somata, along with their distinctive intrinsic electrophysiological properties (Wilson et al., 2004). Specifically, in order to record from PNs, we targeted our electrodes to the cluster of cell bodies immediately anterodorsal to the antennal lobe neuropil, which contains a pure population of uniglomerular PNs (Jefferis et al., 2001; Lai et al., 2008). We confirmed that all these cells had small-amplitude action potentials (<12 mV), which is diagnostic of PNs (Wilson et al., 2004). We also filled a subset of these cells with biocytin and verified that they were PNs based on their

morphology. To record from GABA-LNs, we targeted our electrodes to the cluster of cell bodies lateral to the antennal lobe neuropil. This cluster contains both PNs and GABA-LNs (Jefferis et al., 2001; Lai et al., 2008), but GABA-LNs are easily identifiable on the basis of their large action potentials (>24 mV), again as confirmed by biocytin fills (Wilson and Laurent, 2005a; Wilson et al., 2004; Yaksi and Wilson, 2010). Glu-LN somata are located ventral to the antennal lobe, and so are in a distinctly different location from PN and GABA-LN somata. Glu-LN somata were always targeted for recording based on GFP expression (in *OK371-Gal4,UAS-CD8:GFP* flies), and in a subset of recordings we used biocytin fills to verify that the GFP+ cells we recorded from in this cluster were always antennal lobe LNs. Recordings were performed with an Axopatch 200B amplifier (Axon Instruments). Recorded voltages were low-pass filtered at 5 kHz and digitized at 10 kHz.

Odor stimulation

Odors used were diluted 100-fold in paraffin oil and delivered via a custom-built olfactometer, which further dilutes the headspace of the odor vial 10-fold in air (Olsen et al., 2007). Odor was delivered at a flow rate of 2.2 mL/min. Odor stimuli were applied for 2 s every 30 s, with 5 or 6 trials per stimulus. In one experiment, we observed odor-evoked firing rates that varied >2 fold over the course of the experiment, and we excluded this experiment from further analysis.

Histochemistry

In some experiments, the morphology of the recorded neurons was visualized after recording by incubating the brain with a fluorescent conjugate of streptavidin, as published previously (Wilson et al., 2004). Immunohistochemistry was performed as described previously (Wilson and Laurent, 2005a; Wilson et al., 2004). Primary antibodies were obtained from the

following sources (with dilutions in parentheses): mouse nc82 from the Developmental Studies Hybridoma Bank (1:20) rat anti-CD8 from Invitrogen (1:200), rabbit anti-VGluT from A. DiAntonio (1:500; ref. Daniels et al., 2008), rabbit anti-VGAT from D.E. Krantz (1:200; ref. Fei et al., 2010). Secondary antibodies (Invitrogen) were used at 1:250. To reconstruct neuronal morphology from biocytin fills, we hand-traced the skeletonized morphology using the Simple Neurite Tracer plugin in Fiji, using the Fill Out command to automatically generate a 3D volume, which we subsequently converted to a *z*-projection.

Glutamate and GABA iontophoresis

For glutamate iontophoresis, a high-resistance sharp pulled glass pipette was filled with a solution of 1M monosodium glutamate in water (pH=8). The pipette was placed in the antennal lobe neuropil, and glutamate was ejected using a 10-20 ms negative current pulse applied with an iontophoresis current generator gated by a voltage pulse (Model 260, World Precision Instruments). A constant positive backing current was applied to retain glutamate in the pipette between ejections. The magnitude of the iontophoresis response depends on the placement of the pipette as well as the ejection current magnitude and duration, and these variables were adjusted in each experiment to ensure that the ejection artifact was small. (The artifact is visible as a downward deflection, and flips symmetrically to become an upward deflection when the ejection pulse is inverted.). Because these adjustments are necessarily subjective, in the experiments comparing two genotypes (Fig. 3.3E,F), the experimenter was blinded to genotype. For GABA iontophoresis, the glass pipette was filled with 250 mM GABA in water (pH=4.3). GABA was ejected using a 20 ms positive pulse, and a negative backing current was applied to retain GABA in the pipette between ejections. Tetrodotoxin (1 μM) was added to the bath in all iontophoresis experiments to block network activity.

Stimulation of LNs with ATP/P2X2

We used ATP/P2X2 to stimulate glutamatergic neurons because we found that expression of channelrhodopsin-2 under control of the *OK371-Gal4* driver produced lethality, likely due to basal activity of channelrhodopsin-2 in motorneurons. In our experiments using the ATP/P2X2 system (Lima and Miesenbock, 2005), the ATP ejection pipette was filled with 10 mM MgATP in water and placed near the edge of the antennal lobe neuropil at the base of the ipsilateral antennal nerve (for Glu-LN activation), or at the dorsolateral edge of the antennal lobe neuropil (for GABA-LN activation). The ATP solution was pressure-ejected for 10 ms at 6 psi using a pneumatic device gated by a voltage pulse (PV820, World Precision Instruments). As a negative control, we recorded from Glu-LNs that lacked P2X2 expression (genotype *OK371-Gal4,UAS-CD8:GFP*) and confirmed that they were not depolarized by ATP. As an additional negative control, we also recorded from PNs and GABA-LNs in flies lacking the Gal4 driver (genotype *UAS-CD8:GFP*;*UAS-P2X2*) and confirmed that ATP ejection elicited a negligible response in these cells, which demonstrates that there is no expression of P2X2 in the absence of Gal4. However, if the ejection duration was prolonged beyond 10 ms, or if the pipette was buried in the antennal lobe neuropil, we observed a depolarization evoked by ATP pressure ejection in these control recordings.

Paired recordings

Paired recordings were performed in an *ex vivo* preparation where the brain was removed from the head and immobilized on a coverslip. In order to target Glu-LNs in the paired recordings, we expressed GFP under the control of the *OK371-Gal4* driver. PNs and GABA-LNs were unlabeled, but could be identified based on their soma location, soma size, and spike shape. The presynaptic cell was stimulated by injecting a 500-ms step of depolarizing current. The size

of the step was adjusted to achieve depolarizations > 30 mV in the stimulated cell. Current injections were repeated every 6 s for 30-60 trials. The response of the unstimulated cell was low-pass filtered at 50 Hz and averaged across trials. A pair was defined as connected if the response of the unstimulated cell was > 0.3 mV. In a few cases, we defined a pair as connected even though the response was <0.3 mV, because the response was abolished by a neurotransmitter receptor antagonist (picrotoxin, CGP54626, or mecamylamine). In some pairs, we saw evidence of weak ephaptic coupling. These responses were small (typically <0.2 mV in the unstimulated cell) and had a latency and shape that was very similar to the voltage deflection in the stimulated cell, but in the opposite direction. They were not abolished by tetrodotoxin (1 μM).

Electrical stimulation of ORN axons

Electrical stimulation of the antennal nerve (in Fig. 3.8) was performed essentially as previously described (Kazama and Wilson, 2008). The ipsilateral antennal nerve was severed and drawn into a saline-filled suction electrode. A pair of 50-μs current pulses, 25 ms apart, was delivered to the nerve using a current isolator (A.M.P.I). We discarded trials in which there were unclamped spikes. We also discarded trials in which there were failures in either $EPSC_1$ or $EPSC_2$ (defined as events with an amplitude < 20% of the trial-averaged amplitude for that EPSC). Unitary EPSCs at this synapse are generally highly reliable in their trial-to-trial amplitudes, and so we interpret these failures as failures of axon recruitment, not failures of synaptic vesicle release. Consistent with this interpretation, we could sometimes obtain a more reliable recording by releasing and then re-inserting the nerve into the suction electrode. Because of occasional large fluctuations in EPSC amplitude (likely due to fluctuating recruitment of axons), we only analyzed paired-pulse ratios over a run of trials where recruitment was stable.

Specifically, paired-pulse ratios were measured over the maximum window of consecutive trials where the trial-to-trial coefficient of variation in $EPSC_1$ amplitude was less than 30%, where the minimum number of consecutive trials must be at least six. In these experiments, the iontophoretic ejection current began 400 ms prior to $EPSC_1$ and lasted 50 ms. This protocol ensured that the evoked EPSCs fell within the steady-state of the postsynaptic outward current evoked by glutamate. The postsynaptic outward current evoked by glutamate iontophoresis was on average 6 pA, which was 22% of the average magnitude of $EPSC_1$ (27 pA). Current traces were low pass filtered at 1 kHz prior to digitization at 10 kHz.

Acknowledgements

We thank A. DiAntonio for anti-VGlut antibody, D.E. Krantz for anti-VGAT antibody, G. Miesenböck for *UAS-P2X2* flies, and members of the Wilson lab for feedback on the manuscript. This work was supported by a research project grant from the National Institutes of Health (R01DC008174). W.W.L. is supported by an HHMI International Research Fellowship and a Presidential Scholarship from Harvard Medical School. R.I.W. is an HHMI Early Career Scientist.

CHAPTER 4: Conclusion

Drosophila has emerged as an important experimental system for understanding how specific neurons, circuits, and computations give rise to behavior. The growing use of electrophysiological techniques has enabled us to correlate neural activity with sensory stimuli and probe the mechanisms that give rise to these patterns of neural activity. This is, in large part, due to the development of new genetic tools to label specific neurons and to manipulate and monitor neural activity. While the repertoire of tools for manipulating neural activity is large, techniques for transient inactivation of neurons have been limited. In Chapter 2, I described a novel technique for rapidly silencing *Drosophila* neurons *in vivo* using a native histamine-gated chloride channel (Ort). Taking advantage of the fact that histamine is present only sparsely in the nervous system outside of the eye, and selectively gates a high-conductance chloride channel, we showed that ectopically expressing Ort can effectively block neural activity in several different cell types in the olfactory system. The Ort/histamine system is a promising addition to the *Drosophila* genetic toolkit for probing functional connectivity between identified neurons *in vivo*.

Once key tools are in place, an important next step in understanding neural circuit computations is to identify the physiological effects of neurotransmitters. Among the major neurotransmitters, glutamate has been most extensively studied in contexts where it is excitatory. In *Drosophila*, glutamate is well-known to act as an excitatory neurotransmitter at the neuromuscular junction, but its effects in the central brain are poorly understood. In Chapter 3, I showed that glutamate is an inhibitory neurotransmitter in the *Drosophila* olfactory system, acting through a glutamate-gated chloride channel. The role of glutamate is broadly similar to that of GABA in this circuit, although these neurotransmitters may act on different spatial and

temporal scales. The existence of two parallel inhibitory transmitter systems may increase the range and flexibility of synaptic inhibition.

Together, these studies contribute to a more thorough understanding of how neural circuits encode and process sensory information in the *Drosophila* brain. More broadly, they demonstrate that *Drosophila* can be a useful model for investigating the principles underlying neural circuit function. As we gain a more complete understanding of simpler circuits like that of the fly, it will be exciting to see if similar principles also govern the workings of larger brains.

Bibliography

Barbara, G.S., Zube, C., Rybak, J., Gauthier, M., and Grunewald, B. (2005). Acetylcholine, GABA and glutamate induce ionic currents in cultured antennal lobe neurons of the honeybee, Apis mellifera. J Comp Physiol A Neuroethol Sens Neural Behav Physiol *191*, 823-836.

Bellen, H.J., D'Evelyn, D., Harvey, M., and Elledge, S.J. (1992). Isolation of temperature-sensitive diphtheria toxins in yeast and their effects on Drosophila cells. Development *114*, 787-796.

Benzer, S. (1973). Genetic dissection of behavior. Scientific American *229*, 24-37.

Berdnik, D., Chihara, T., Couto, A., and Luo, L. (2006). Wiring stability of the adult Drosophila olfactory circuit after lesion. The Journal of neuroscience : the official journal of the Society for Neuroscience *26*, 3367-3376.

Berni, J., Pulver, S.R., Griffith, L.C., and Bate, M. (2012). Autonomous circuitry for substrate exploration in freely moving Drosophila larvae. Curr Biol *22*, 1861-1870.

Cao, G., Platisa, J., Pieribone, V.A., Raccuglia, D., Kunst, M., and Nitabach, M.N. (2013). Genetically targeted optical electrophysiology in intact neural circuits. Cell *154*, 904-913.

Chalasani, S.H., Chronis, N., Tsunozaki, M., Gray, J.M., Ramot, D., Goodman, M.B., and Bargmann, C.I. (2007). Dissecting a circuit for olfactory behaviour in Caenorhabditis elegans. Nature *450*, 63-70.

Charron, F., and Tessier-Lavigne, M. (2007). The Hedgehog, TGF-beta/BMP and Wnt families of morphogens in axon guidance. Advances in experimental medicine and biology *621*, 116-133.

Chou, Y.H., Spletter, M.L., Yaksi, E., Leong, J.C., Wilson, R.I., and Luo, L. (2010a). Diversity and wiring variability of olfactory local interneurons in the Drosophila antennal lobe. Nat Neurosci *13*, 439-449.

Chou, Y.H., Spletter, M.L., Yaksi, E., Leong, J.C., Wilson, R.I., and Luo, L. (2010b). Diversity and wiring variability of olfactory local interneurons in the Drosophila antennal lobe. Nat Neurosci *13*, 439-449.

Clark, D.A., Bursztyn, L., Horowitz, M.A., Schnitzer, M.J., and Clandinin, T.R. (2011). Defining the computational structure of the motion detector in Drosophila. Neuron *70*, 1165-1177.

Cleland, T.A. (1996). Inhibitory glutamate receptor channels. Mol Neurobiol *13*, 97-136.

Collins, B., Kane, E.A., Reeves, D.C., Akabas, M.H., and Blau, J. (2012). Balance of activity between LN(v)s and glutamatergic dorsal clock neurons promotes robust circadian rhythms in Drosophila. Neuron *74*, 706-718.

Cully, D.F., Paress, P.S., Liu, K.K., Schaeffer, J.M., and Arena, J.P. (1996). Identification of a Drosophila melanogaster glutamate-gated chloride channel sensitive to the antiparasitic agent avermectin. J Biol Chem *271*, 20187-20191.

Daniels, R.W., Gelfand, M.V., Collins, C.A., and DiAntonio, A. (2008). Visualizing glutamatergic cell bodies and synapses in *Drosophila* larval and adult CNS. J Comp Neurol *508*, 131-152.

Das, A., Chiang, A., Davla, S., Priya, R., Reichert, H., VijayRaghavan, K., and Rodrigues, V. (2011a). Identification and analysis of a glutamatergic local interneuron lineage in the adult Drosophila olfactory system. Neural Syst Circuits *1*, 4.

Das, S., Sadanandappa, M.K., Dervan, A., Larkin, A., Lee, J.A., Sudhakaran, I.P., Priya, R., Heidari, R., Holohan, E.E., Pimentel, A., *et al.* (2011b). Plasticity of local GABAergic interneurons drives olfactory habituation. Proc Natl Acad Sci U S A *108*, E646-654.

Devaud, J.M., Clouet-Redt, C., Bockaert, J., Grau, Y., and Parmentier, M.L. (2008). Widespread brain distribution of the Drosophila metabotropic glutamate receptor. Neuroreport *19*, 367-371.

Dietzl, G., Chen, D., Schnorrer, F., Su, K.C., Barinova, Y., Fellner, M., Gasser, B., Kinsey, K., Oppel, S., Scheiblauer, S., *et al.* (2007). A genome-wide transgenic RNAi library for conditional gene inactivation in Drosophila. Nature *448*, 151-156.

Fei, H., Chow, D.M., Chen, A., Romero-Calderon, R., Ong, W.S., Ackerson, L.C., Maidment, N.T., Simpson, J.H., Frye, M.A., and Krantz, D.E. (2010). Mutation of the Drosophila vesicular GABA transporter disrupts visual figure detection. J Exp Biol *213*, 1717-1730.

Fenno, L., Yizhar, O., and Deisseroth, K. (2011). The development and application of optogenetics. Annu Rev Neurosci *34*, 389-412.

Foelix, R.F., Stocker, R.F., and Steinbrecht, R.A. (1989). Fine structure of a sensory organ in the arista of Drosophila melanogaster and some other dipterans. Cell and tissue research *258*, 277-287.

Gaiano, N. (2008). Strange bedfellows: Reelin and Notch signaling interact to regulate cell migration in the developing neocortex. Neuron *60*, 189-191.

Gallio, M., Ofstad, T.A., Macpherson, L.J., Wang, J.W., and Zuker, C.S. (2011). The coding of temperature in the Drosophila brain. Cell *144*, 614-624.

Gengs, C., Leung, H.T., Skingsley, D.R., Iovchev, M.I., Yin, Z., Semenov, E.P., Burg, M.G., Hardie, R.C., and Pak, W.L. (2002). The target of Drosophila photoreceptor synaptic transmission is a histamine-gated chloride channel encoded by ort (hclA). J Biol Chem *277*, 42113-42120.

Gonzalez-Bellido, P.T., Wardill, T.J., Kostyleva, R., Meinertzhagen, I.A., and Juusola, M. (2009). Overexpressing temperature-sensitive dynamin decelerates phototransduction and bundles microtubules in Drosophila photoreceptors. The Journal of neuroscience : the official journal of the Society for Neuroscience *29*, 14199-14210.

Gouwens, N.W., and Wilson, R.I. (2009). Signal propagation in Drosophila central neurons. J Neurosci *29*, 6239-6249.

Hamada, F.N., Rosenzweig, M., Kang, K., Pulver, S.R., Ghezzi, A., Jegla, T.J., and Garrity, P.A. (2008). An internal thermal sensor controlling temperature preference in Drosophila. Nature *454*, 217-220.

Hamasaka, Y., Rieger, D., Parmentier, M.L., Grau, Y., Helfrich-Forster, C., and Nassel, D.R. (2007). Glutamate and its metabotropic receptor in Drosophila clock neuron circuits. J Comp Neurol *505*, 32-45.

Hardie, R.C. (1989). A histamine-activated chloride channel involved in neurotransmission at a photoreceptor synapse. Nature *339*, 704-706.

Hiesinger, P.R., Zhai, R.G., Zhou, Y., Koh, T.W., Mehta, S.Q., Schulze, K.L., Cao, Y., Verstreken, P., Clandinin, T.R., Fischbach, K.F., *et al.* (2006). Activity-independent prespecification of synaptic partners in the visual map of Drosophila. Current biology : CB *16*, 1835-1843.

Ho, K.S., and Scott, M.P. (2002). Sonic hedgehog in the nervous system: functions, modifications and mechanisms. Current opinion in neurobiology *12*, 57-63.

Huang, J., Zhang, W., Qiao, W., Hu, A., and Wang, Z. (2010). Functional connectivity and selective odor responses of excitatory local interneurons in Drosophila antennal lobe. Neuron *67*, 1021-1033.

Inada, K., Kohsaka, H., Takasu, E., Matsunaga, T., and Nose, A. (2011). Optical dissection of neural circuits responsible for Drosophila larval locomotion with halorhodopsin. PloS one *6*, e29019.

Isaacson, J.S., and Scanziani, M. (2011). How inhibition shapes cortical activity. Neuron *72*, 231-243.

Jefferis, G.S., Marin, E.C., Stocker, R.F., and Luo, L. (2001). Target neuron prespecification in the olfactory map of Drosophila. Nature *414*, 204-208.

Joesch, M., Schnell, B., Raghu, S.V., Reiff, D.F., and Borst, A. (2010). ON and OFF pathways in Drosophila motion vision. Nature *468*, 300-304.

Kazama, H., and Wilson, R.I. (2008). Homeostatic matching and nonlinear amplification at genetically-identified central synapses. Neuron *58*, 401-413.

Kazama, H., and Wilson, R.I. (2009). Origins of correlated activity in an olfactory circuit. Nat Neurosci *12*, 1136-1144.

Kitamoto, T. (2001). Conditional modification of behavior in Drosophila by targeted expression of a temperature-sensitive shibire allele in defined neurons. J Neurobiol *47*, 81-92.

Kitamoto, T. (2002). Targeted expression of temperature-sensitive dynamin to study neural mechanisms of complex behavior in Drosophila. J Neurogenet *16*, 205-228.

Kosaka, T., and Ikeda, K. (1983). Reversible blockage of membrane retrieval and endocytosis in the garland cell of the temperature-sensitive mutant of Drosophila melanogaster, shibirets1. The Journal of cell biology *97*, 499-507.

Kunes, S., and Steller, H. (1991). Ablation of Drosophila photoreceptor cells by conditional expression of a toxin gene. Genes & development *5*, 970-983.

Lai, S.L., Awasaki, T., Ito, K., and Lee, T. (2008). Clonal analysis of Drosophila antennal lobe neurons: diverse neuronal architectures in the lateral neuroblast lineage. Development *135*, 2883-2893.

Lechner, H.A., Lein, E.S., and Callaway, E.M. (2002). A genetic method for selective and quickly reversible silencing of Mammalian neurons. J Neurosci *22*, 5287-5290.

Lee, T., and Luo, L. (1999). Mosaic analysis with a repressible cell marker for studies of gene function in neuronal morphogenesis. Neuron *22*, 451-461.

Lerchner, W., Xiao, C., Nashmi, R., Slimko, E.M., van Trigt, L., Lester, H.A., and Anderson, D.J. (2007). Reversible silencing of neuronal excitability in behaving mice by a genetically targeted, ivermectin-gated Cl- channel. Neuron *54*, 35-49.

Lima, S.Q., and Miesenbock, G. (2005). Remote control of behavior through genetically targeted photostimulation of neurons. Cell *121*, 141-152.

Littleton, J.T., and Ganetzky, B. (2000). Ion channels and synaptic organization: analysis of the Drosophila genome. Neuron *26*, 35-43.

Littleton, J.T., Stern, M., Perin, M., and Bellen, H.J. (1994). Calcium dependence of neurotransmitter release and rate of spontaneous vesicle fusions are altered in Drosophila synaptotagmin mutants. Proceedings of the National Academy of Sciences of the United States of America *91*, 10888-10892.

Luo, L., Callaway, E.M., and Svoboda, K. (2008). Genetic dissection of neural circuits. Neuron *57*, 634-660.

Ma, Q. (2010). Labeled lines meet and talk: population coding of somatic sensations. The Journal of clinical investigation *120*, 3773-3778.

Magnus, C.J., Lee, P.H., Atasoy, D., Su, H.H., Looger, L.L., and Sternson, S.M. (2011). Chemical and genetic engineering of selective ion channel-ligand interactions. Science *333*, 1292-1296.

Mahr, A., and Aberle, H. (2006). The expression pattern of the Drosophila vesicular glutamate transporter: a marker protein for motoneurons and glutamatergic centers in the brain. Gene expression patterns : GEP *6*, 299-309.

Masse, N.Y., Turner, G.C., and Jefferis, G.S. (2009). Olfactory information processing in Drosophila. Curr Biol *19*, R700-713.

McCarthy, E.V., Wu, Y., Decarvalho, T., Brandt, C., Cao, G., and Nitabach, M.N. (2011). Synchronized bilateral synaptic inputs to *Drosophila melanogaster* neuropeptidergic rest/arousal neurons. J Neurosci *31*, 8181-8193.

Miyashita, T., Oda, Y., Horiuchi, J., Yin, J.C., Morimoto, T., and Saitoe, M. (2012). Mg(2+) block of Drosophila NMDA receptors is required for long-term memory formation and CREB-dependent gene expression. Neuron *74*, 887-898.

Moffat, K.G., Gould, J.H., Smith, H.K., and O'Kane, C.J. (1992). Inducible cell ablation in Drosophila by cold-sensitive ricin A chain. Development *114*, 681-687.

Montell, C., Jones, K., Hafen, E., and Rubin, G. (1985). Rescue of the Drosophila phototransduction mutation trp by germline transformation. Science *230*, 1040-1043.

Nassel, D.R. (1999). Histamine in the brain of insects: a review. Microsc Res Tech *44*, 121-136.

Ng, M., Roorda, R.D., Lima, S.Q., Zemelman, B.V., Morcillo, P., and Miesenbock, G. (2002). Transmission of olfactory information between three populations of neurons in the antennal lobe of the fly. Neuron *36*, 463-474.

Ni, L., Bronk, P., Chang, E.C., Lowell, A.M., Flam, J.O., Panzano, V.C., Theobald, D.L., Griffith, L.C., and Garrity, P.A. (2013). A gustatory receptor paralogue controls rapid warmth avoidance in Drosophila. Nature *500*, 580-584.

Nitabach, M.N., Blau, J., and Holmes, T.C. (2002). Electrical silencing of Drosophila pacemaker neurons stops the free-running circadian clock. Cell *109*, 485-495.

Olsen, S.R., Bhandawat, V., and Wilson, R.I. (2007). Excitatory interactions between olfactory processing channels in the Drosophila antennal lobe. Neuron *54*, 89-103.

Olsen, S.R., Bhandawat, V., and Wilson, R.I. (2010). Divisive normalization in olfactory population codes. Neuron *66*, 287-299.

Olsen, S.R., and Wilson, R.I. (2008a). Lateral presynaptic inhibition mediates gain control in an olfactory circuit. Nature *452*, 956-960.

Olsen, S.R., and Wilson, R.I. (2008b). Lateral presynaptic inhibition mediates gain control in an olfactory circuit. Nature *452*, 956-960.

Pantazis, A., Segaran, A., Liu, C.H., Nikolaev, A., Rister, J., Thum, A.S., Roeder, T., Semenov, E., Juusola, M., and Hardie, R.C. (2008). Distinct roles for two histamine receptors (hclA and hclB) at the Drosophila photoreceptor synapse. J Neurosci *28*, 7250-7259.

Panula, P., Happola, O., Airaksinen, M.S., Auvinen, S., and Virkamaki, A. (1988). Carbodiimide as a tissue fixative in histamine immunohistochemistry and its application in developmental neurobiology. J Histochem Cytochem *36*, 259-269.

Paradis, S., Sweeney, S.T., and Davis, G.W. (2001). Homeostatic control of presynaptic release is triggered by postsynaptic membrane depolarization. Neuron *30*, 737-749.

Parmentier, M.L., Pin, J.P., Bockaert, J., and Grau, Y. (1996). Cloning and functional expression of a Drosophila metabotropic glutamate receptor expressed in the embryonic CNS. J Neurosci *16*, 6687-6694.

Pollack, I., and Hofbauer, A. (1991). Histamine-like immunoreactivity in the visual system and brain of Drosophila melanogaster. Cell Tissue Res *266*, 391-398.

Prescott, S.A., and Ratte, S. (2012). Pain processing by spinal microcircuits: afferent combinatorics. Current opinion in neurobiology *22*, 631-639.

Pulver, S.R., Pashkovski, S.L., Hornstein, N.J., Garrity, P.A., and Griffith, L.C. (2009). Temporal dynamics of neuronal activation by Channelrhodopsin-2 and TRPA1 determine behavioral output in Drosophila larvae. J Neurophysiol *101*, 3075-3088.

Raghu, S.V., and Borst, A. (2011). Candidate glutamatergic neurons in the visual system of Drosophila. PLoS One *6*, e19472.

Ramaekers, A., Parmentier, M.L., Lasnier, C., Bockaert, J., and Grau, Y. (2001). Distribution of metabotropic glutamate receptor DmGlu-A in Drosophila melanogaster central nervous system. J Comp Neurol *438*, 213-225.

Raymond, V., Sattelle, D.B., and Lapied, B. (2000). Co-existence in DUM neurones of two GluCl channels that differ in their picrotoxin sensitivity. Neuroreport *11*, 2695-2701.

Richmond, J.E., and Broadie, K.S. (2002). The synaptic vesicle cycle: exocytosis and endocytosis in Drosophila and C. elegans. Current opinion in neurobiology *12*, 499-507.

Rister, J., Pauls, D., Schnell, B., Ting, C.Y., Lee, C.H., Sinakevitch, I., Morante, J., Strausfeld, N.J., Ito, K., and Heisenberg, M. (2007). Dissection of the peripheral motion channel in the visual system of Drosophila melanogaster. Neuron *56*, 155-170.

Root, C.M., Masuyama, K., Green, D.S., Enell, L.E., Nassel, D.R., Lee, C.H., and Wang, J.W. (2008). A presynaptic gain control mechanism fine-tunes olfactory behavior. Neuron *59*, 311-321.

Salkoff, L., Baker, K., Butler, A., Covarrubias, M., Pak, M.D., and Wei, A. (1992). An essential 'set' of K+ channels conserved in flies, mice and humans. Trends in neurosciences *15*, 161-166.

Scanziani, M. (2000). GABA spillover activates postsynaptic GABA(B) receptors to control rhythmic hippocampal activity. Neuron *25*, 673-681.

Shang, Y., Claridge-Chang, A., Sjulson, L., Pypaert, M., and Miesenbock, G. (2007). Excitatory local circuits and their implications for olfactory processing in the fly antennal lobe. Cell *128*, 601-612.

Silbering, A.F., and Galizia, C.G. (2007). Processing of odor mixtures in the Drosophila antennal lobe reveals both global inhibition and glomerulus-specific interactions. J Neurosci *27*, 11966-11977.

Silbering, A.F., Rytz, R., Grosjean, Y., Abuin, L., Ramdya, P., Jefferis, G.S., and Benton, R. (2011). Complementary function and integrated wiring of the evolutionarily distinct Drosophila olfactory subsystems. J Neurosci *31*, 13357-13375.

Simpson, J.H. (2009). Mapping and manipulating neural circuits in the fly brain. Adv Genet *65*, 79-143.

Skingsley, D.R., Laughlin, S.B., and Hardie, R.C. (1995). Properties of histamine-activated chloride channels in the large monopolar cells of the dipteran compound eye: a comparative study. J Comp Physiol [A] *176*, 611-623.

Slimko, E.M., McKinney, S., Anderson, D.J., Davidson, N., and Lester, H.A. (2002). Selective electrical silencing of mammalian neurons in vitro by the use of invertebrate ligand-gated chloride channels. J Neurosci *22*, 7373-7379.

Staley, K.J., Soldo, B.L., and Proctor, W.R. (1995). Ionic mechanisms of neuronal excitation by inhibitory GABAA receptors. Science *269*, 977-981.

Stocker, R.F. (1994). The organization of the chemosensory system in Drosophila melanogaster: a review. Cell and tissue research *275*, 3-26.

Stocker, R.F., Heimbeck, G., Gendre, N., and de Belle, J.S. (1997). Neuroblast ablation in Drosophila P[GAL4] lines reveals origins of olfactory interneurons. J Neurobiol *32*, 443-456.

Stocker, R.F., Lienhard, M.C., Borst, A., and Fischbach, K.F. (1990a). Neuronal architecture of the antennal lobe in Drosophila melanogaster. Cell and tissue research *262*, 9-34.

Stocker, R.F., Lienhard, M.C., Borst, A., and Fischbach, K.F. (1990b). Neuronal architecture of the antennal lobe in Drosophila melanogaster. Cell Tissue Res *262*, 9-34.

Stocker, R.F., Singh, R.N., Schorderet, M., and Siddiqi, O. (1983). Projection patterns of different types of antennal sensilla in the antennal glomeruli of Drosophila melanogaster. Cell and tissue research *232*, 237-248.

Sudhakaran, I.P., Holohan, E.E., Osman, S., Rodrigues, V., Vijayraghavan, K., and Ramaswami, M. (2012). Plasticity of recurrent inhibition in the Drosophila antennal lobe. J Neurosci *32*, 7225-7231.

Sweeney, L.B., Couto, A., Chou, Y.H., Berdnik, D., Dickson, B.J., Luo, L., and Komiyama, T. (2007). Temporal target restriction of olfactory receptor neurons by Semaphorin-1a/PlexinA-mediated axon-axon interactions. Neuron *53*, 185-200.

Sweeney, S.T., Broadie, K., Keane, J., Niemann, H., and O'Kane, C.J. (1995). Targeted expression of tetanus toxin light chain in Drosophila specifically eliminates synaptic transmission and causes behavioral defects. Neuron *14*, 341-351.

Takemura, S.Y., Karuppudurai, T., Ting, C.Y., Lu, Z., Lee, C.H., and Meinertzhagen, I.A. (2011). Cholinergic circuits integrate neighboring visual signals in a Drosophila motion detection pathway. Curr Biol *21*, 2077-2084.

Tanaka, N.K., Endo, K., and Ito, K. (2012). Organization of antennal lobe-associated neurons in adult Drosophila melanogaster brain. The Journal of comparative neurology *520*, 4067-4130.

Tempel, B.L., Papazian, D.M., Schwarz, T.L., Jan, Y.N., and Jan, L.Y. (1987). Sequence of a probable potassium channel component encoded at Shaker locus of Drosophila. Science *237*, 770-775.

Thum, A.S., Knapek, S., Rister, J., Dierichs-Schmitt, E., Heisenberg, M., and Tanimoto, H. (2006). Differential potencies of effector genes in adult Drosophila. J Comp Neurol *498*, 194-203.

Tian, L., Hires, S.A., Mao, T., Huber, D., Chiappe, M.E., Chalasani, S.H., Petreanu, L., Akerboom, J., McKinney, S.A., Schreiter, E.R., *et al.* (2009). Imaging neural activity in worms, flies and mice with improved GCaMP calcium indicators. Nature methods *6*, 875-881.

van der Bliek, A.M., and Meyerowitz, E.M. (1991). Dynamin-like protein encoded by the Drosophila shibire gene associated with vesicular traffic. Nature *351*, 411-414.

Venken, K.J., Simpson, J.H., and Bellen, H.J. (2011). Genetic manipulation of genes and cells in the nervous system of the fruit fly. Neuron *72*, 202-230.

Vosshall, L.B., and Stocker, R.F. (2007). Molecular architecture of smell and taste in Drosophila. Annu Rev Neurosci *30*, 505-533.

Wang, J.W., Wong, A.M., Flores, J., Vosshall, L.B., and Axel, R. (2003). Two-photon calcium imaging reveals an odor-evoked map of activity in the fly brain. Cell *112*, 271-282.

Warmke, J.W., and Ganetzky, B. (1994). A family of potassium channel genes related to eag in Drosophila and mammals. Proceedings of the National Academy of Sciences of the United States of America *91*, 3438-3442.

Wilson, R.I. (2011). Understanding the functional consequences of synaptic specialization: insight from the Drosophila antennal lobe. Curr Opin Neurobiol *21*, 254-260.

Wilson, R.I., and Laurent, G. (2005a). Role of GABAergic inhibition in shaping odor-evoked spatiotemporal patterns in the Drosophila antennal lobe. J Neurosci *25*, 9069-9079.

Wilson, R.I., and Laurent, G. (2005b). Role of GABAergic inhibition in shaping odor-evoked spatiotemporal patterns in the Drosophila antennal lobe. J Neurosci *25*, 9069-9079.

Wilson, R.I., Turner, G.C., and Laurent, G. (2004). Transformation of olfactory representations in the Drosophila antennal lobe. Science *303*, 366-370.

Wu, C.L., Xia, S., Fu, T.F., Wang, H., Chen, Y.H., Leong, D., Chiang, A.S., and Tully, T. (2007). Specific requirement of NMDA receptors for long-term memory consolidation in Drosophila ellipsoid body. Nat Neurosci *10*, 1578-1586.

Wulff, P., Goetz, T., Leppa, E., Linden, A.M., Renzi, M., Swinny, J.D., Vekovischeva, O.Y., Sieghart, W., Somogyi, P., Korpi, E.R., *et al.* (2007). From synapse to behavior: rapid modulation of defined neuronal types with engineered GABAA receptors. Nat Neurosci *10*, 923-929.

Xia, S., Miyashita, T., Fu, T.F., Lin, W.Y., Wu, C.L., Pyzocha, L., Lin, I.R., Saitoe, M., Tully, T., and Chiang, A.S. (2005). NMDA receptors mediate olfactory learning and memory in *Drosophila*. Curr Biol *15*, 603-615.

Yaksi, E., and Wilson, R.I. (2010). Electrical coupling between olfactory glomeruli. Neuron *67*, 1034-1047.

Yao, Z., Macara, A.M., Lelito, K.R., Minosyan, T.Y., and Shafer, O.T. (2012). Analysis of functional neuronal connectivity in the Drosophila brain. J Neurophysiol *108*, 684-696.

Zhang, Y.Q., Rodesch, C.K., and Broadie, K. (2002). Living synaptic vesicle marker: synaptotagmin-GFP. Genesis *34*, 142-145.

Zheng, Y., Hirschberg, B., Yuan, J., Wang, A.P., Hunt, D.C., Ludmerer, S.W., Schmatz, D.M., and Cully, D.F. (2002). Identification of two novel Drosophila melanogaster histamine-gated chloride channel subunits expressed in the eye. J Biol Chem *277*, 2000-2005.

Zhou, L., Schnitzler, A., Agapite, J., Schwartz, L.M., Steller, H., and Nambu, J.R. (1997). Cooperative functions of the reaper and head involution defective genes in the programmed cell death of Drosophila central nervous system midline cells. Proceedings of the National Academy of Sciences of the United States of America *94*, 5131-5136.

Zucker, R.S., and Regehr, W.G. (2002). Short-term synaptic plasticity. Annu Rev Physiol *64*, 355-405.